



Contents lists available at ScienceDirect

Journal of Traditional and Complementary Medicine

journal homepage: <http://www.elsevier.com/locate/jtcme>

Transcriptome and metabolome changes induced by bitter melon (*Momordica charantia*)- intake in a high-fat diet induced obesity model



Dominique Reed^a, Dileep Kumar^a, Sushil Kumar^b, Komal Raina^{a,c}, Reenu Punia^a, Rama Kant^a, Laura Saba^a, Charmion Cruickshank-Quinn^a, Boris Tabakoff^a, Nichole Reisdorph^a, Michael G. Edwards^d, Michael Wempe^a, Chapla Agarwal^{a,e}, Rajesh Agarwal^{a,e,*}

^a Department of Pharmaceutical Sciences, Skaggs School of Pharmacy and Pharmaceutical Sciences, University of Colorado Anschutz Medical Campus, Aurora, CO, USA

^b Division of Critical Care Medicine and Cardiovascular Pulmonary Research, Departments of Pediatrics and Medicine, University of Colorado Anschutz Medical Campus, Aurora, CO, USA

^c Department of Pharmaceutical Sciences, College of Pharmacy and Allied Health Professions, South Dakota State University, Brookings, SD, USA

^d Bioinfo Solutions LLC, Parker, CO, USA

^e University of Colorado Cancer Center, University of Colorado Anschutz Medical Campus, Aurora, CO, USA

ARTICLE INFO

Article history:

Received 22 July 2021

Received in revised form

16 August 2021

Accepted 16 August 2021

Available online 19 August 2021

Keywords:

Bitter melon

Momordica charantia

Metabolic syndrome

High fat diet-induced obesity

Diet intervention

ABSTRACT

Background and aim: Metabolic syndrome (MetS) is a complex disease of physiological imbalances interrelated to abnormal metabolic conditions, such as abdominal obesity, type II diabetes, dyslipidemia and hypertension. In the present pilot study, we investigated the nutraceutical bitter melon (*Momordica charantia* L) -intake induced transcriptome and metabolome changes and the converging metabolic signaling networks underpinning its inhibitory effects against MetS-associated risk factors.

Experimental procedure: Metabolic effects of lyophilized bitter melon juice (BMJ) extract (oral gavage 200 mg/kg/body weight-daily for 40 days) intake were evaluated in diet-induced obese C57BL/6J male mice [fed-high fat diet (HFD), 60 kcal% fat]. Changes in *a*) serum levels of biochemical parameters, *b*) gene expression in the hepatic transcriptome (microarray analysis using Affymetrix Mouse Exon 1.0 ST arrays), and *c*) metabolite abundance levels in lipid-phase plasma [liquid chromatography mass spectrometry (LC-MS)-based metabolomics] after BMJ intervention were assessed.

Results and conclusion: BMJ-mediated changes showed a positive trend towards enhanced glucose homeostasis, vitamin D metabolism and suppression of glycerophospholipid metabolism. In the liver, nuclear peroxisome proliferator-activated receptor (PPAR) and circadian rhythm signaling, as well as bile acid biosynthesis and glycogen metabolism targets were modulated by BMJ ($p < 0.05$). Thus, our in-depth transcriptomics and metabolomics analysis suggests that BMJ-intake lowers susceptibility to the onset of high-fat diet associated MetS risk factors partly through modulation of PPAR signaling and its

Abbreviations: MetS, Metabolic syndrome; BMJ, bitter melon juice; DIO, diet-induced obese; HFD, high fat diet; HDL, high density lipoprotein (cholesterol); LDL, low density lipoprotein (cholesterol); PC, phosphatidylcholine; PE, phosphatidylethanolamine; AMPK, adenosine monophosphate-activated protein kinase; PPARs, Peroxisome proliferator-activated receptors; LC-MS, liquid-chromatography mass spectrometry; HMDB, Human Metabolome Database; KEGG, Kyoto Encyclopedia of Genes and Genomes.

* Corresponding author. Department of Pharmaceutical Sciences, Skaggs School of Pharmacy and Pharmaceutical Sciences, University of Colorado Anschutz Medical Campus, 12850 E. Montview Blvd, C238, Room V20-2118, Aurora, CO, 80045, USA.

E-mail address: Rajesh.Agarwal@cuanschutz.edu (R. Agarwal).

Peer review under responsibility of The Center for Food and Biomolecules, National Taiwan University.

<https://doi.org/10.1016/j.jtcme.2021.08.011>

2225-4110/© 2021 Center for Food and Biomolecules, National Taiwan University. Production and hosting by Elsevier Taiwan LLC. This is an open access article under the CC BY-NC-ND license (<http://creativecommons.org/licenses/by-nc-nd/4.0/>).

downstream targets in circadian rhythm processes to prevent excessive lipogenesis, maintain glucose homeostasis and modify immune responses signaling.

© 2021 Center for Food and Biomolecules, National Taiwan University. Production and hosting by Elsevier Taiwan LLC. This is an open access article under the CC BY-NC-ND license (<http://creativecommons.org/licenses/by-nc-nd/4.0/>).

1. Introduction

Metabolic syndrome (MetS) is widely recognized as a condition that arises from the combined onset of multiple metabolic disorders, such as obesity, dyslipidemia, glucose intolerance, hypertension/stroke, diabetes and cardiovascular disease.^{1–3} According to the statistics reported by the Centers for Disease Control and Prevention, several major risk factors of MetS, such as cardiovascular disease, stroke and diabetes are ranked among the top ten leading causes of mortality in the United States (US).⁴ Diagnosis and treatment of MetS has been a challenge due to the multiple traits of this disease. The National Cholesterol Education Program Adult Treatment Panel III (NCEP-ATP III),^{5,6} CardioMetabolic Health Alliance Staging system,⁷ and International Diabetes Foundation (IDF)⁸ have developed diagnosis criteria widely used to diagnose MetS.⁹ However, a global consensus has not been reached on this criterion.

Precision nutrition focused preventive and therapeutic regimens show promise as alternative approaches for the management of MetS.^{10–14} In this regard, the use of nutraceutical such as *Momordica charantia* L. (bitter gourd or bitter melon fruit), a member of the Cucurbitaceae family,¹⁵ has been shown to lessen symptoms associated with aberrant metabolic conditions.^{16–22} The plant of bitter melon is a climber and bears oblong fruits (cucumber shaped); the young fruits are emerald/green in color and on ripening turn to orange-yellow.¹⁵ Bitter melon fruit, as well as its other parts, have been used in traditional medicine against insulin resistance, hyperlipidemia, hyperglycemia, inflammation and other conditions in Asian, African and Caribbean cultures.^{15–17,23,24} The MetS improving properties of bitter melon have been attributed to a mixture of phytochemicals such as, steroidal saponins (e.g. charantin), alkaloid (vicine), polypeptide-p (referred to as plant insulin), other cucurbitane-type triterpenoids (momordicosides) and α -eleostearic acid.^{15,25} In recent scientific reports, the metabolic regulatory, anti-diabetic and anti-lipidemic effects of bitter melon and its constituents have been recognized in glucose and lipid metabolism.^{18–20,26–28} These effects have been verified in diet-induced obese (DIO) murine studies,^{16,17,29,30} where bitter melon intake has been linked to the improvement in insulin sensitivity, plasma high-density lipoprotein (HDL) levels and modulation of immune response signaling.¹⁶ In obesity-associated inflammation, bitter melon has been shown to exert a suppressive effect against inflammation as evidenced by its reduction of serum cytokine levels and macrophage/mast cell recruitment in adipose tissue in DIO mice.¹⁷

Recent clinical trials have also shown several health benefits of bitter melon against MetS and other associated conditions.^{18–20} Different preparations of bitter melon significantly reduced fasting plasma glucose levels of type II diabetic¹⁸ and pre-diabetic patients.¹⁹ MetS incidence was decreased by 7.1% after lyophilized wild bitter melon consumption (4.8 g) in Taiwanese adults (after 3 months) in an open-label uncontrolled supplementation trial.²⁰ These pre-clinical and clinical studies demonstrate the potential of bitter melon to control and improve exacerbated immune responses, abnormal metabolism of glucose and lipids in MetS.

On the other hand, our laboratory studies have shown that pancreatic cancer effects of bitter melon are mediated via

modulation of phosphoinositide 3 and Akt serine/threonine kinase signaling (which are critical to glucose homeostasis and other metabolic mechanisms).^{23,24,31–33} Taken together, literature on these signaling pathways show that bitter melon primarily, 1) is a key activator of AMPK (adenosine monophosphate-activated protein kinase) and PPARs (Peroxisome proliferator-activated receptors) [α/γ], and 2) rebalances lipid and glucose metabolism, and 3) attenuates metabolic abnormalities. In the present pilot study, we investigated bitter melon-intake induced transcriptome and metabolome changes and the converging metabolic signaling networks underpinning its inhibitory effects against MetS-associated risk factors.

2. Materials and methods

2.1. Serum biochemical profiling kits

Relevant Colorimetric or Fluorometric Assay kits were used to determine the serum levels ($n = 4/\text{group}$) of Glucose [Cayman Chemicals, Ann Arbor, MI, USA (# 10009582)], Triglyceride [Abcam, Cambridge, MA, USA (# ab65336)]; Total Cholesterol [Cayman Chemicals (# 10007640)]; High-density (HDL), low-density (LDL), very low density (VLDL) lipoprotein levels [Abcam (# ab65390)]; Leptin [Invitrogen, Carlsbad, CA, USA (# KM C2281)] and Adiponectin [Abcam (# ab108785)].

2.2. Bitter melon juice (BMJ) extraction and storage

BMJ was extracted from commercially available Chinese variety of bitter melon fruit (*Momordica Charantia*) and a standardized lyophilized preparation was prepared as described previously.^{23,24,31} The smooth green-Chinese variety used in the study have a characteristic pebbly surface with smooth length wise ridges. Briefly, bitter melon fruit, after discarding seeds and pulp, is juiced using a juicer, and the juice centrifuged at $3000 \times g$ at 4°C for 30 min. Under aseptic conditions, BMJ is vacuum filtered (corning cellulose acetate filter, $0.22 \mu\text{m}$), stirred for homogeneity and dispensed (10–12 mL) into 20 mL Wheaton serum vials for batch lyophilization using a SMART cycle on a Lyostar3 (FTS Systems SP Scientific) system. Prior to vial closure, containers are back sealed with N₂; using this method, presently we have already standardized the procedure to typically obtain about 260 vials per batch starting with 10 lbs of Chinese green bitter melon that gives 300 mL BMJ/lb fruit and 340 mg lyophilized BMJ powder/10 mL BMJ. All these steps are well standardized. An advantage of bulk process, producing many sealed vials, is that it allows us to systematically conduct long-term stability and storage studies over an extended time-period to further ensure quality control and to avoid batch-to-batch variations.

2.3. Bitter Melon Juice extract-dietary intervention study

Sixteen-week-old diet-induced obese (DIO) C57BL/6J male mice [fed-high fat diet (HFD), 60 kcal% fat from Research diets Inc., New Brunswick, NJ, USA (#D12492)] from 4 weeks of age] were purchased from Jackson labs (Bar Harbor, ME, USA). The D12492 diet

formulation contains Proteins (20% Kcal) as Casein, Lactic-30 mesh (200 g) and Cystine, L (3 g); Carbohydrates (20% Kcal) as Lodex 10 (125 g) and Sucrose-fine granulated (72.8 g); Fiber as Solka Floc, FCC200 (50 g); Fat (60% Kcal) as Lard (245 g) and Soybean oil-USP (25 g); Mineral-S10026B (50 g); Vitamins as Choline Bitartrate (2 g) and V10001C (1 g); the diet appears blue due to addition of Blue FD&C, Alum Lake (35–42%: 0.05 g) in a total diet weight of 773.85 g. The energy density is 5.21 Kcal/g.

Once received at the animal house facility in the University of Colorado Denver [Anschutz Medical Campus (AMC), Aurora, CO, USA], the DIO mice were randomized into two groups ($n = 4/\text{group}$): a) Control-DIO group maintained on the 60 kcal% HFD for additional 40 days, and b) BMJ + DIO group also maintained on 60 kcal% HFD fat for additional 40 days plus oral gavage with lyophilized bitter melon juice extract [(200 mg/kg body weight/day), reconstituted in sterile deionized water immediately before use, and given as total volume of 100 μL per mouse at 11:00 a.m. daily] throughout the study. On similar lines, the Control-DIO group was also subjected to oral gavage with vehicle only (100 μL sterile deionized water) throughout the duration of the study. Throughout the course of the study, mice had water ad libitum; weight of the mice and diet-intake was measured twice weekly and mice were monitored daily for their general health. On day 40 of study initiation, mice in both groups were subjected to fasting for 6 h and then sacrificed after CO_2 asphyxiation and exsanguination. Blood was collected and plasma/serum stored for biochemical/metabolic assessments. Liver was weighed, a portion fixed in formalin for histopathological processing while another portion was flash frozen in liquid nitrogen and stored in -80°C for measuring RNA expression levels. The study was conducted according to the guidelines of the Declaration of Helsinki, and the animal treatment protocol was approved by the Institutional Animal Care and Use Committee of the University of Colorado Denver-AMC Protocol # 57913(04)1E.

2.4. Microarray analysis

RNA extraction from frozen livers ($n = 3/\text{group}$) stored in RNAlater solution (Life Technologies, Carlsbad, CA, USA) of both DIO and BMJ + DIO groups and nucleic acid clean-up were performed using RNeasy plus Universal and RNeasy Mini kits (Qiagen, Germantown, MD, USA) according to the manufacturer's instructions, respectively. RNA was converted to cDNA and hybridized to separate Affymetrix Mouse Exon 1.0 ST arrays (Santa Clara, CA, USA) according to manufacturer's recommendations.³⁴ Expression estimates and detection above background p-values for individual genes were estimated using Affymetrix Power Tools and the RMA-sketch algorithm.³⁵ Probe sets were grouped into gene clusters using ensembl gene annotation (GRCm38 version 89). A probe set was included in a gene cluster if all of its associated probes aligned to a region completely contained within the exonic region of the transcript.

2.5. Liquid chromatography mass spectrometry

Plasma collected from DIO and BMJ + DIO groups ($n = 3/\text{group}$) were subjected to untargeted liquid-chromatography mass spectrometry (LC-MS)-based metabolomics.^{36,37} Briefly, each sample (100 μL) was subjected to protein precipitation using methanol, followed by liquid-liquid extraction using methyl-tert butyl ether as previously described^{38,39} to obtain an aqueous fraction and a lipid fraction. The lipid fraction was dried down and resuspended in 100% methanol for LC-MS analysis. The samples from the lipid fraction were injected on to an Agilent Zorbax Rapid Resolution HD (RRHD) SB-C18, 1.8 μm (2.1×100 mm) analytical column and an

Agilent Zorbax SB-C18, 1.8 μm (2.1×5 mm) guard column attached to an Agilent 1290 series pump. The autosampler tray temperature was set at 4°C , column temperature was set at 60°C , and the sample injection volume was 4 μL . The flow rate was 0.7 mL/min with the following mobile phases: mobile phase A was water with 0.1% formic acid, and mobile phase B was 60:36:4 isopropyl alcohol:acetonitrile:water with 0.1% formic acid. Gradient elution was as follows: 0–1 min 30–70% B, 1–7.92 min 70–100% B, 7.92–10.4 min 100% B, 10.4–10.5 min 100–30% B, followed by column re-equilibration with 30% B from 10.5 to 15.1 min. The mass spectrometry conditions were as follows: Agilent 6210 Time-of-Flight mass spectrometer (TOF-MS) in positive ionization mode with dual electrospray (ESI) source, mass range 60–1600 m/z , scan rate 2.03, gas temperature 300°C , gas flow 12.0L/min, nebulizer 30psi, skimmer 60V, capillary voltage 4000V, fragmentor 120V, reference masses 121.050873 and 922.009798 (Agilent reference mix). Given that Agilent 6210 is a TOF and not a QTOF MS, the accurate mass and retention time (AMRT) library was built on a 6520 QTOF comprising the same LC parameters and very similar MS parameters to the 6210 while also incorporating MSMS at 10, 20, and 40 eV. This AMRT library was built using >600 known standards from the Iroa MSMLS, as well as in-house standards for other small molecules and lipids not currently present in the MSMLS. Comparing these known standards across both MS platforms, the retention time shift was in a range of 0.1–0.5 min across years and different lots of the same HPLC column type. As such, this AMRT library built from MSMS and RT of standards could be used on the 6210 data files for an added degree of confidence in compound names.

2.6. Metabolomics data extraction and annotation

A plasma sample randomly selected from one of the mice was prepared as described above for use as a quality control (QC) sample to monitor instrument reproducibility over the run batch for a total of 5 injections. Total ion chromatograms of all samples were evaluated for retention time reproducibility and intensity overlap. Instrument QC samples were analyzed to ensure that peak areas of spiked internal standards in the plasma samples were reproducible with coefficient of variations $\leq 10\%$. Compounds were extracted in MassHunter Profinder B.06 (Agilent Technologies, Santa Clara, CA, USA) using the Batch Recursive Feature Extraction workflow. The Molecule Feature Extraction conditions were as follows: Retention time range 0.25–10 min. Ion species H^+ , Na^+ , K^+ , charge state 1–2, two or more ions, retention time window 0.2 min, height >1000 counts, MFE score 80, and compounds must be present in at least 2 samples. The ion parameters were as follows: retention time window 0.2 min, peak height >1000 counts, and compounds must be present in at least 2 sample files.⁴⁰

Metabolites were annotated in Mass Profiler Professional software v14.5 using an in-house mass and retention time library consisting of >700 authentic standards.^{41,42} The remaining compounds were matched to an in-house database comprising data from Human Metabolome Database (HMDB), Kyoto Encyclopedia of Genes and Genomes (KEGG) and LIPID Metabolites and Pathways Strategy (LIPID MAPS) using isotope ratios, chemical formulas, database scores and a mass error window of ≤ 10 ppm. Metabolite abundance levels, retention time, mass and chemical formulas were exported from these databases using Mass Profiler.⁴³

2.7. LC-MS chemicals, standards and reagents

All solvents were LC-MS grade. Water and isopropyl alcohol were purchased from Honeywell Burdick & Jackson (Muskegon, MI, USA); chloroform, acetonitrile, methanol, acetic acid, low retention

microcentrifuge tubes, serological pipettes were purchased from Fisher Scientific (Fair Lawn, NJ, USA); plastic pipette tips were purchased from USA Scientific (Orlando, FL, USA); methyl *tert*-butyl ether was purchased from J.T. Baker (Central City, PA, USA); internal standards were purchased from Avanti Polar lipids Inc. and Sigma Aldrich (St. Louis, MO, USA); pyrex glass culture tubes were purchased from Corning Incorporated (Corning, NY, USA).

2.8. Gene and metabolite functional enrichment analysis

To enable functional interpretation of experimental data, enrichment analyses were performed using *in silico* platforms. Protein and pathway associations were predicted based on gene ontology (GO), and KEGG pathway using web-based Enrichr tool,^{44,45} STITCH.⁴⁶ Enrichment of gene profiles were correlated to target disease phenotypes (Disease Atlas) and compounds (Pharmac Atlas) using an analogous Gene Set Enrichment Analysis (GSEA) method (Illumina BaseSpace Correlation Engine, San Diego, CA, USA).⁴⁷ Enrichment analysis of LC-MS metabolomic data was performed via HMDB, KEGG and LIPID MAPS databases to predict the biological role, chemical classification and associated pathways using the Metabolite Biological Role 2.0 (MBRole 2.0)⁴⁸ tool.

2.9. Statistical analysis

Microarray gene expression differences in the two study groups (BMJ + DIO vs. DIO) above background in at least 3 samples was included in the differential expression analysis ($\pm 1.2 \geq$ ratio; DABG $p < 0.0001$) and were determined using the empirical Bayes method to stabilize variance estimates in the limma package of R (R version 3.2.3).⁴⁹ All statistical analyses of animal experimental data collected from BMJ + DIO and DIO study groups were determined either by unpaired Student's *t*-test or one-way analysis of variance ($p \leq 0.05$) followed by adjustment for multiple hypothesis testing carried out with Sigma Stat software version 2.03 (Jandel Scientific, San Rafael, CA, USA). Statistical analyses of Enrichr and STITCH protein and pathway associations were determined by unadjusted *p*-value values ($p \leq 0.05$), the false discovery rate (FDR) method ($FDR \leq 0.05$), confidence range (low: <0.4 , medium: 0.4 to 0.7 , high: >0.7), and combined scores. Illumina BaseSpace analyses of gene expression data between the two study groups (BMJ + DIO vs. DIO) determined related disease phenotypes and compounds with similar activity using *p*-values computed by the Fisher's exact test. Statistical difference in metabolite abundance levels ($\pm 1.2 \geq$ fold change) in the BMJ + DIO (treatment) and DIO (control) study groups were determined by unpaired Student's *t*-test ($p \leq 0.05$) followed by $FDR \leq 0.05$ using the Mass Profiler Professional software v14.5. MBROLE computes the statistical significance of each annotation in a set of metabolite compounds based on a random set of the same size from the background set using unpaired Student's *t*-test and $FDR \leq 0.05$.

3. Results

3.1. Modulatory effect of BMJ on diet-induced obese state

To understand the metabolic effect of bitter melon on diet-associated obesity (a major MetS risk factor), DIO C57BL/6J male mice fed on a HFD were subjected to oral administration of BMJ extract (200 mg/kg per body weight) for 40 days. HFD-induced obesity in this mice model is associated with metabolic aberrations (though HFD may not necessarily induce hyperglycemia), i.e., insulin resistance, hyperinsulinemia, impaired glucose intolerance, hyperlipidemia, and hypertriglyceridemia. Importantly, after BMJ intervention, the increase in body weight gain from baseline

(intervention study initiation-day 0) was relatively less compared to untreated DIO controls (Fig. 1A, Supplemental Table 1). It is noteworthy that there was no decrease in body weight in BMJ + DIO group compared to baseline weights of DIO mice, which indicated that BMJ could not reverse the effects of HFD diet on weight gain, but BMJ could slow down the weight gain in the presence of continued exposure to HFDs (there was no difference in diet intake). In line with this observation, the mean liver weight in BMJ + DIO group was ~24% less than DIO controls (Fig. 1B; though the difference was not statistically significant; $p = 0.19$). On gross appearance, the livers of DIO mice had a buff/fatty-creamy appearance, while livers from BMJ + DIO group appeared normal. To confirm whether this decrease in liver weight had any pathological manifestations, we compared the histopathology of hepatic tissue from both mice groups. As shown in Fig. 1B, irrespective of treatment, the hepatic tissue in both groups had fatty deposits and showed signs of non-alcoholic fatty liver disease with steatosis; comparatively, the BMJ + DIO hepatic tissues displayed less aggressive signs of steatosis.

Importantly, in accordance with previous studies^{16–21,29} on bitter melon response to MetS risk factors, in the present study BMJ also improved metabolic profiles of DIO mice. Serum glucose ($p = 0.01$) and triglyceride levels ($p = 0.04$) were significantly lowered by ~26–42% in BMJ + DIO group compared to DIO controls (Fig. 1C, Supplemental Table 1). While total cholesterol was not significantly decreased by BMJ intervention, the increase in HDL levels was statistically significant ($p < 0.02$) (Fig. 1C, Supplemental Table 1). Notably, the LDL to HDL ratio was decreased by ~35% in BMJ + DIO group. Relative to DIO mice, serum leptin was decreased by 28% and adiponectin showed a 1.27-fold up-regulation ($p = 0.05$, for both) in the serum of BMJ-fed DIO mice (Fig. 1C, Supplemental Table 1).

3.2. BMJ modulates circadian rhythm via Ppar signaling in hepatic metabolism

Previously, bitter melon supplementation has been shown to counteract metabolic abnormalities^{16,17,26,27,30} in murine models and humans by decreasing lipogenesis and improving insulin sensitivity to glucose as a compensatory response. To determine metabolic signaling changes associated with BMJ intake during DIO state, the gene expression levels of over 20,000 transcripts were evaluated in RNA extracted from the liver of DIO mice (with and without BMJ intervention) via microarray analysis (Fig. 2). Changes were observed in 759 ($\pm 1.2 \geq$ ratio; 20% increase) and 183 ($\pm 1.5 \geq$ ratio change; 50% increase) transcripts in the liver of BMJ-treated DIO mice compared to untreated DIO controls based on $p \leq 0.05$ (Fig. 2 and Supplemental Table 2).

Pathway enrichment of the hepatic transcriptome of BMJ + DIO mice identified 11 pathways with KEGG database ($p < 0.05$) and 124 biological process of GO ($p < 0.05$) involved in metabolic regulation compared to DIO controls via the Enrichr tools as shown in Tables 1 and 2 and Supplemental Table 3. Importantly, hepatic genes (536 up-regulated and 223 down-regulated) by at least ± 1.2 -fold in BMJ + DIO mice were shown to be involved in circadian rhythmic processes (*Cry1*, *Nr1d1*, *Per2*, *Per3*, *Rorc*) via *Ppara* (*Acs1l*, *Cpt1a*, *Cyp4a32*), and *Ppar* (*Cyp7a1*) signaling. BMJ targeted gluconeogenesis (*Cry1*, *Per2*), glucose transport (*Trib3*), glycogen metabolism (*Gys2*, *Nr1d1*, *Per2*), and insulin resistance (*Cpt1a*, *Gys2*, *Insr*, *Ppp1r3b*, *Ppp1r3e*, *Trib3*, *Pik3r1*), that influence glycemic responses as shown in Tables 1 and 2. Notably, circadian rhythm signaling was identified as a target of BMJ regulation in both KEGG and GO pathways in Table 1 and Supplemental Table 3. Also, peroxisome signaling (*Ppar*), a major regulatory pathway in metabolism, was significantly modulated in the livers of BMJ + DIO mice. Nuclear

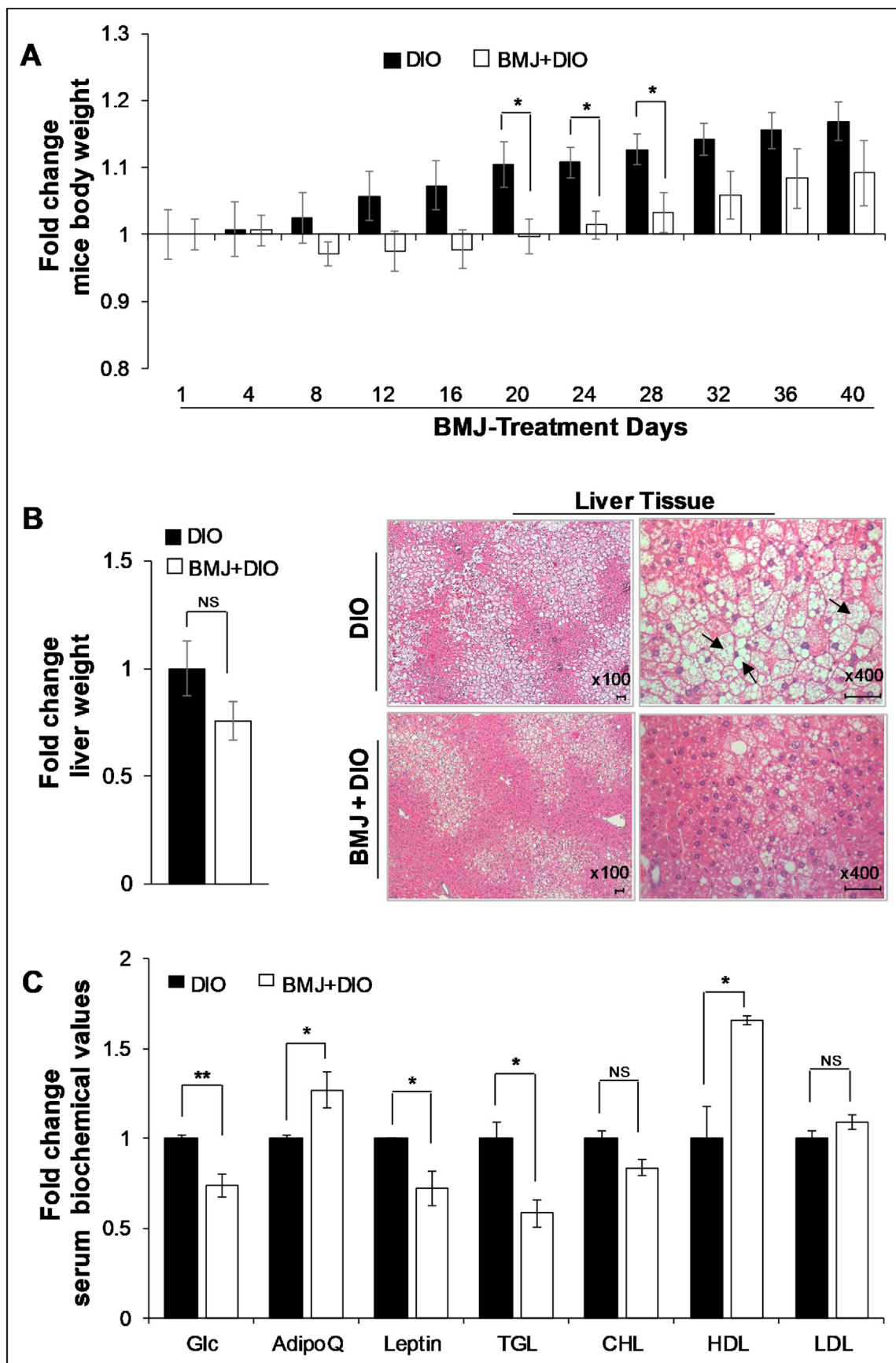


Fig. 1. Body and liver weight changes, and biochemical profile in Bitter Melon Juice (BMJ)-treated high fat diet-induced obese (DIO) C57BL/6J mice. **A)** Relative body weight changes in DIO vs. BMJ + DIO mice. **B)** Relative liver weights of DIO vs. BMJ + DIO mice (left panel); Representative pictographs (x100) of hematoxylin and eosin (H&E) stained hepatic tissue;

receptors, *Ppar α* and *Ppar γ* , have been shown to directly regulate circadian rhythm signaling—which in turn is associated with the metabolism of glucose, lipid, and Vitamin D.^{50–52} BMJ intervention exhibited modulation of hepatic expression of glucose homeostasis associated targets, such as insulin receptor (*Insr*) and glycogen synthase 2 (*Gys2*), and also genes associated with cholesterol metabolism and fatty acid oxidation in BMJ + DIO mice compared to the control DIO group. Lipogenic-related targets were altered in BMJ + DIO mice compared to control DIO mice. Transcript levels of fat cell differentiation targets (*Il11*, *Hmga2*, *Ffar2*, *Sox8*, *Inhbb*, *Gdf6*) were reduced by ~17–29% in BMJ + DIO mice compared to control DIO mice. However, BMJ + DIO mice showed an up-regulation ratio ranging from 1.21 to 2.76 of browning-beiging (*Aco2*, *Cyca*, *Slc25a20*, *Fam195a*, *Cox7a2l/Cox7rp*, *Ahcyl1*) and adipose tissue targets (*Dgat2*, *Rorc*). Also, homeostasis and metabolism of triglyceride (*Dgat2*, *Nr1h4*, *Fitm2*), glycerophospholipid (*Gde1*, *Lcat*, *Pigl*, *Enpp6*, *Gpcpd1*, *Plcb1*, *Pla2g7*, *Gpld1*) and cholesterol (*Angptl4*, *Cyp7a1*, *Lcat*, *Npc1*, *Osbpl5*) were also shown to be affected by BMJ intervention against DIO (Supplemental Table 3, Fig. 3). Apart from hepatic genes altered by BMJ in primary metabolic processes, innate/humoral immunity targets were also modulated (Supplemental Table 3). BMJ induced expression changes in the immune response pathways such as complement and coagulation cascade (*C2*, *C4a*, *C4b*, *C8a*, *C8b*, *C9*, *Cfi*, *C5ar1*, *F11*, *Masp1*, *Masp2*) in innate immunity, acute/humoral (*C4a*, *C8a*, *C8b*, *C9*, *Cfi*, *Fcgr2b*, *Ffar2*, *Il6st*), apoptotic cell clearance (*C4a*, *Ccl2*), interleukin 6 associated genes (*Ccl2*, *Il1r1*, *Il6ra*, *Il6st*, *Il15ra*) and serum adipocytokines (leptin, adiponectin) in DIO mice (Supplemental Tables 2–3).

3.3. Correlation of diseases and nutraceutical agents' efficacy with BMJ effect on Metabolism

Next, we used the Illumina BaseSpace Correlation Engine platform (Tables 3 and 4, Supplemental Table 4) to determine a) disease phenotypes related to metabolic dysregulation (Disease Atlas), and b) other natural products and/or bioactive agents which have a similar effect on hepatic gene expression as BMJ (Pharmaco Atlas). Nutraceutical and/or pharmacological agents that correlate with BMJ-associated gene expression were evaluated in DIO mice using the Pharmaco Atlas. BMJ-mediated effects correlated with 787 agents and as expected a strong relationship was shown with anti-inflammatory, antibiotic, anti-lipogenic, anti-cytotoxic, anti-diabetic and estrogen-like agents. For the top 30 ranked agents, over 50% positively correlated with BMJ effects shown in Table 4. Moreover, these agents have shown activities associated with anti-prostaglandin (ibuprofen), inhibition of angiotensin II-increased protein synthesis (trilinolein), anti-diabetic (genipin), anti-tumor (cryptoxanthin), anti-microbial (cefuroxime), anti-inflammatory (fluocinolone acetonide, prednisone, 1-(2-cyano-3,12-dioxooleana-1,9-dien-28-oyl) imidazole, betamethasone), anti-cholesterol (fenofibrate), and estrogen agonism (butylbenzylphthalate).

Through the Disease Atlas analysis, the top 10 phenotypes related to BMJ + DIO gene profiles were identified in MetS-related diseases including heart, vascular, cancer, nutritional and metabolic diseases (Table 4). Of these studies, the data sets of HFD (52 studies), obesity (12 studies), heart disease (12 studies) and cardiovascular disease (19 studies) phenotypes negatively correlated with BMJ effect on the associated gene profiles in our study as shown in Table 4 (Supplemental Table 4). Interestingly, this same

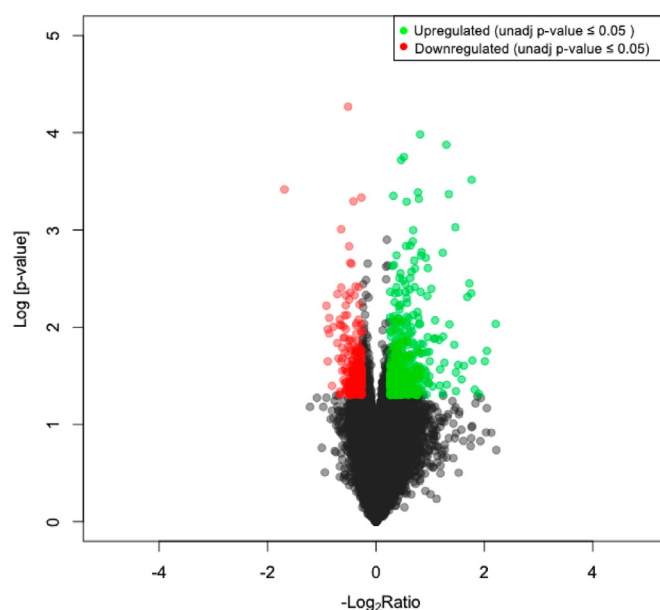


Fig. 2. Volcano plot of differential hepatic gene expression in Bitter Melon Juice (BMJ)-treated high fat diet-induced obese (DIO) C57BL/6J mice. Over 20,000 transcripts were profiled from mouse liver via microarray. A total of 768 genes were differentially expressed by ± 1.2 -ratio ($p \leq 0.05$). Transcriptome profiling showed 535 were up-regulated (red) and 223 were down-regulated (green) in BMJ + DIO mice compared to DIO controls. $n = 4$ per group.

effect was observed in relation to cancer gene targets also.

3.4. Changes in plasma metabolite levels post-BMJ administration in diet induced obese Mice

To further examine the metabolic effects of BMJ, metabolomic profiling was performed on the lipid phase of plasma collected from DIO mice (with and without BMJ intervention) using LC-MS to identify circulating metabolites affected by BMJ intervention (Figs. 3–4). Out of 464 database matched metabolites detected by LC-MS, 36 metabolites were significantly different in BMJ + DIO mice relative to DIO controls ($\pm 1.2 \geq$ fold change; $FDR \leq 0.05$). However, only 36.1% of these 36 metabolites were annotated following database searches, as shown in Table 5. For the remaining 23 metabolites, the chemical formulas, mass and retention time were determined for all but 3 metabolites, which are indicated by mass and retention time only (Supplemental Table 5).

BMJ primarily down-regulated plasma levels of phospholipids, phosphatidylcholine (PC) [PC(20:4_20:4), PC(22:6_20:4)], phosphatidylethanolamine/PE [PE(18:1), PE(18:1) isomer], phosphatidylserine (PS) [PS(17:1)], vitamin D derivatives (25-azavitamin D₃, 2- α -(benzyloxy)-1 α ,25-dihydroxy-19-norvitamin D₃), canavalioid, 13-deoxytedanolide and feticaric acid in BMJ + DIO mice relative to DIO controls (Table 5). Plasma metabolites, DG/DAG/diacylglycerol 40:1, an intermediate of triglyceride, and PE(22:6) exhibited the highest increase in abundance (>4 -fold change) in BMJ + DIO mice (Table 5).

Several plasma metabolites involved in lipid metabolism were affected by BMJ intervention. The pathway and chemical classifications of BMJ targeted metabolites in DIO mice were identified via Metabolite Biological Role analysis (MBRole 2.0). These metabolites

magnified images depicted at $\times 400$ magnification highlight the appearance of fatty globules/steatosis (right panel). Arrows indicate bulging cells with large globules filled with lipid content; scale bar: 50 μ m (C) Relative serum levels of metabolic parameters and adipokines in DIO vs. BMJ + DIO mice. BMJ was given for 40 days as oral gavage: 200 mg/kg body wt). DIO, diet-induced obesity; Glc, glucose; TGA, triglycerides; AdipoQ, Adiponectin. ** $p < 0.02$; * $p < 0.05$. $n = 4$ per group.

Table 1

Bitter melon Juice (BMJ)-treated high fat diet (HFD)-induced obese (DIO) C57BL/6J mice Liver Transcriptome Enrichment Analysis. Signaling pathways were identified from differentially expressed genes in the liver of BMJ + DIO mice via KEGG and Panther pathway enrichment analyses (unadjusted p-value ≤ 0.05). Genes involved in 2 or more KEGG pathways are depicted in bold print. n = 4 per group.

Pathway	p-value	Genes
Complement and coagulation cascades	1.33E-04	C4b ;C4bp;C9; Cfi ;C5ar1;F11; Masp2 ; Masp1 ;Hc;C8b;C8a; C2
Primary bile acid biosynthesis	2.71E-03	Acot8 ; Amacr ; Cyp7a1 ; Slc27a5
Insulin resistance	3.37E-03	Gys2; Slc27a1 ; Cpt1a ;Creb3l3;Pp1r3b;Ppp1r3e;Insr;Trib3;Pik3r1; Slc27a2 ; Slc27a5
Staphylococcus aureus infection	3.51E-03	C4b ;Fcgr4; Cfi ;C5ar1;Defb1; Masp2 ; Masp1 ;Hc;Fcgr2b; C2
RNA polymerase	3.88E-03	Polr2b;Polr1a;Polr1b;Polr3f;Polr2l
Peroxisome	4.88E-03	Acot8 ;Pex19; Amacr ; Acs11 ;Pex11a;Mpv17l;Pxmp4; Slc27a2 ;Ddo
Circadian rhythm	5.29E-03	Per2;Per3;Rorc;Cry1;Nr1d1
Prion diseases	9.10E-03	Hspa5;C9;Hc;C8b;C8a
PPAR signaling	1.63E-02	Slc27a1 ; Cpt1a ; Acs11 ;Cyp4a32; Angptl4 ; Slc27a2 ; Cyp7a1 ; Slc27a5
Choline metabolism in cancer	3.67E-02	Slc22a3; Slc22a5 ;Slc44a2;Dgka;Pik3r1;Plcg1;Plpp3;Gpcpd1
Cholesterol metabolism	3.91E-02	Npc1;Osbp15;Lcat; Angtl4 ; Cyp7a1

Table 2

Metabolic-associated pathways and genes in Bitter Melon Juice (BMJ)-treated high fat diet (HFD)- induced obese (DIO) mice. Changes in KEGG pathway-associated hepatic gene expression after BMJ treatment (unadjusted p-value≤0.05). Genes involved in 2 or more KEGG pathways are depicted in bold print. n = 4 per group.

Pathway	Gene	Ratio	p-value	FDR	
Complement and coagulation cascades	C2	1.24	3.98E-02	5.72E-01	
	C4b	1.35	3.74E-02	5.72E-01	
	C4bp	1.37	3.98E-02	5.72E-01	
	C5ar1	1.23	3.57E-02	5.72E-01	
	C8a	1.74	2.52E-02	5.72E-01	
	C8b	1.91	1.80E-02	5.72E-01	
	C9	1.52	3.28E-02	5.72E-01	
	Cfi	1.54	4.89E-02	5.72E-01	
	F11	1.40	3.30E-02	5.72E-01	
	Hc	1.65	3.43E-02	5.72E-01	
	Masp1	1.32	4.77E-02	5.72E-01	
	Masp2	1.26	4.72E-02	5.72E-01	
	Primary bile acid biosynthesis	Acot8	1.27	1.93E-02	5.72E-01
		Amacr	1.25	3.27E-02	5.72E-01
Cyp7a1		1.95	2.47E-03	5.72E-01	
Slc27a5		1.29	4.89E-02	5.72E-01	
Insulin resistance		Cpt1a	1.26	2.54E-02	5.72E-01
	Creb3l3	1.34	4.41E-03	5.72E-01	
	Gys2	1.47	1.98E-02	5.72E-01	
	Insr	1.42	4.47E-02	5.72E-01	
	Pik3r1	1.42	4.16E-02	5.72E-01	
	Ppp1r3b	1.59	1.90E-02	5.72E-01	
	Ppp1r3e	1.43	2.92E-02	5.72E-01	
	Slc27a1	1.31	1.55E-02	5.72E-01	
	Slc27a2	1.24	4.11E-02	5.72E-01	
	Slc27a5	1.30	4.89E-02	5.72E-01	
	Trib3	0.83	2.77E-02	5.72E-01	
	Circadian rhythm	Cry1	1.53	3.57E-02	5.72E-01
		Nr1d1	0.31	3.83E-04	5.72E-01
		Per2	1.46	4.34E-03	5.72E-01
Per3		1.43	1.77E-04	5.72E-01	
Rorc		2.76	9.39E-04	5.72E-01	
PPAR signaling		Acs11	1.55	3.12E-03	5.72E-01
	Angptl4	1.27	3.62E-02	5.72E-01	
	Cpt1a	1.26	2.54E-02	5.72E-01	
	Cyp4a32	2.27	2.71E-02	5.72E-01	
	Cyp7a1	1.95	2.47E-03	5.72E-01	
	Slc27a1	1.31	1.55E-02	5.72E-01	
	Slc27a2	1.24	4.11E-02	5.72E-01	
	Slc27a5	1.29	4.89E-02	5.72E-01	
	Cholesterol metabolism	Angptl4	1.27	3.62E-02	5.72E-01
		Cyp7a1	1.95	2.47E-03	5.72E-01
Lcat		1.23	4.69E-02	5.72E-01	
Npc1		1.39	4.57E-02	5.72E-01	
Osbp15		1.26	4.11E-02	5.72E-01	

were predicted to function in phospholipid metabolism (i.e., glycerophospholipid, linoleic acid metabolism), glycerophospholipid metabolism/phospholipid biosynthesis (i.e., phosphatidylcholine, phosphatidylserine, and phosphatidylethanolamine biosynthesis), adaptive immunity (B cell receptor, T cell receptor) and

adipocytokine (adiponectin, leptin, DG 40:1) signaling were modified by BMJ treatment (FDR≤0.05) as shown in Fig. 3 and Supplemental Table 7. The biological roles of these metabolites were identified as nutrients, membrane stability, cellular fuel and/or energy sources (Supplemental Table 6).

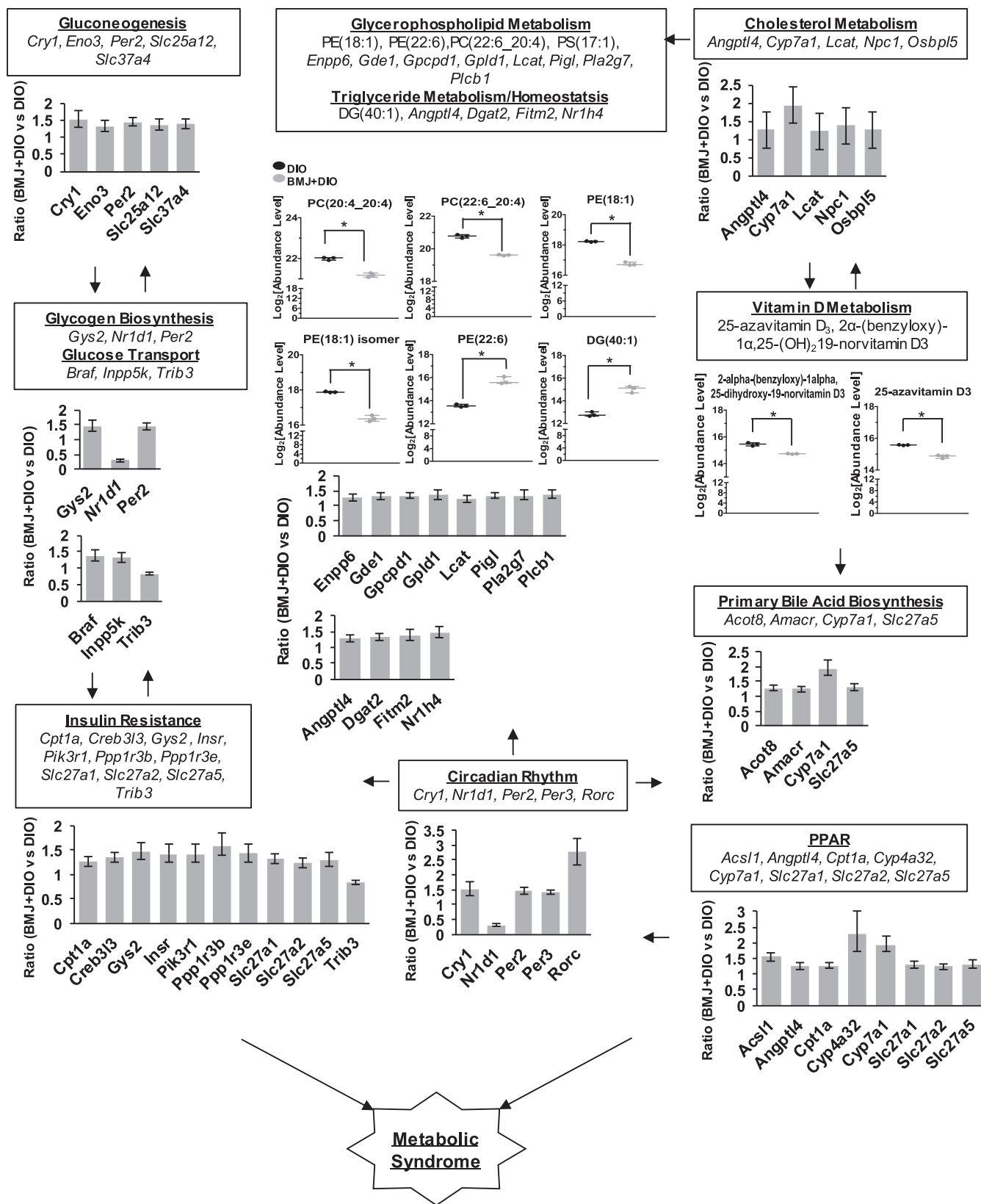


Fig. 3. Bitter Melon Juice (BMJ) targeted signaling pathways in Metabolic Syndrome (MetS). Transcriptome and metabolome analyses identified several signaling pathways that contribute to metabolic syndrome (MetS). Major risk factors of metabolic syndrome include cardiovascular disease, obesity, type II diabetes, dyslipidemia, hypertension and vitamin D deficiency. BMJ treatment changed hepatic gene expression ($*p \leq 0.05$) and plasma metabolites ($*FDR \leq 0.05$) involved in circadian rhythmic regulation, peroxisome proliferator-activated receptor (PPAR) signaling, apoptosis, insulin resistance, glycerophospholipid, cholesterol and vitamin D metabolism that affect MetS risk factors ($*FDR \leq 0.05$).

Table 3

Top 30 compounds that correlate with Bitter Melon Juice (BMJ) effect in high fat diet (HFD)- induced obese (DIO) C57BL/6J mice liver transcriptome. Differentially expressed transcripts in hepatic RNA extracted from BMJ + DIO mice (unadjusted p-value ≤ 0.05) were imported into the BaseSpace correlation engine by Illumina. Top 30 highly correlated compounds are displayed in the table. The Pharmaco Atlas genomic application tool identified compounds and treatments that correlate with gene expression data based on public genomic data sources.

Compound	Compound Group	# of Studies	Correlation	Illumina Score
Okadaic Acid	Membrane Transport Modulators/Enzyme Inhibitors	1	negative	100.00
Ethylnitrosourea	Alkylating Agents	1	negative	96.33
Cefuroxime	Unclassified Mechanisms of Action	1	positive	90.60
Trilinolein	Unclassified Mechanisms of Action	2	positive	88.67
Cryptoxanthin	Unclassified Mechanisms of Action	1	positive	86.44
Aflatoxins	Unclassified Mechanisms of Action	1	negative	84.40
1-(2-cyano-3,12-dioxoleano-1,9-dien-28-oyl) imidazole	Unclassified Mechanisms of Action	1	positive	84.35
Genipin	Unclassified Mechanisms of Action	1	positive	83.58
Butylbenzyl phthalate	Unclassified Mechanisms of Action	1	positive	81.59
Thioacetamide	Unclassified Mechanisms of Action	14	negative	80.13
Malathion	Enzyme Inhibitors/Neurotransmitter Agents	2	negative	79.46
Heptachlor Epoxide	Unclassified Mechanisms of Action	1	negative	78.94
Senecionine	Unclassified Mechanisms of Action	1	negative	76.54
Methapyrilene	Neurotransmitter Agents	12	negative	74.13
N-nitrosomorpholine	Unclassified Mechanisms of Action	1	negative	73.61
Naphthalene	Unclassified Mechanisms of Action	2	negative	73.29
Colchicine	Mitosis Modulators	8	negative	72.52
Ibuprofen	Unclassified Mechanisms of Action	2	positive	72.31
Miconazole	Enzyme Inhibitors	8	negative	71.66
Cyanoginosin LR	Enzyme Inhibitors	3	negative	71.54
Prednisone	Unclassified Mechanisms of Action	5	positive	71.22
Tunicamycin	Unclassified Mechanisms of Action	8	negative	71.17
Phenacetin	Unclassified Mechanisms of Action	7	positive	70.88
Fluocinolone Acetonide	Unclassified Mechanisms of Action	6	positive	70.74
Hexachlorobenzene	Unclassified Mechanisms of Action	1	negative	70.65
Betamethasone	Unclassified Mechanisms of Action	3	positive	70.58
Pristane	Unclassified Mechanisms of Action	2	negative	70.50
Fenofibrate	Unclassified Mechanisms of Action	20	positive	70.06
Direct black 3	Unclassified Mechanisms of Action	1	positive	69.95
Dimethylnitrosamine	Unclassified Mechanisms of Action	8	negative	69.77

Table 4

MetS-related disease phenotypes in Bitter melon Juice (BMJ) treated high fat diet (HFD)- induced obese (DIO) C57BL/6J mice liver transcriptome. Differentially expressed transcripts in hepatic RNA extracted from BMJ + DIO mice were imported into the BaseSpace correlation engine by Illumina. Highly correlated phenotypes were selected from among the top 3 Metabolic Syndrome (MetS)-related disease groups. The Disease Atlas genomic application tool identified disease traits, conditions and experimental endpoints based on public genomic data sources that correlate with gene expression data based on public genomic data sources (unadjusted p-value ≤ 0.05).

Phenotypes group	Phenotype	# of Studies	Correlation	Illumina Score
Nutritional and Metabolic Diseases	High fat diet	52	negative	95.91
Nutritional and Metabolic Diseases	Alpha-1-antitrypsin deficiency	1	negative	92.45
Nutritional and Metabolic Diseases	Deficiency state	29	positive	84.07
Nutritional and Metabolic Diseases	Ketogenic diet	2	positive	82.47
Nutritional and Metabolic Diseases	Hypophosphatasia	2	positive	82.29
Nutritional and Metabolic Diseases	Hypoalphalipoproteinemia	3	positive	82.15
Nutritional and Metabolic Diseases	Ischemic reperfusion injury	7	negative	80.53
Nutritional and Metabolic Diseases	Renal carnitine transport defect	1	positive	79.13
Nutritional and Metabolic Diseases	Argininosuccinate lyase deficiency	2	positive	77.76
Nutritional and Metabolic Diseases	Obesity	12	negative	70.37
Cancer	Liver cancer	71	negative	94.08
Cancer	Thyroid cancer	14	negative	68.75
Cancer	Lung cancer	53	negative	66.49
Cancer	Gastric cancer	23	negative	66.24
Cancer	Kidney cancer	24	negative	65.47
Cancer	Malignant tumor of intestine	52	negative	64.35
Cancer	Adrenal cancer	5	negative	64.22
Cancer	Brain cancer	40	negative	63.49
Cancer	Malignant tumor of muscle	14	negative	62.82
Cancer	Pancreatic cancer	9	positive	42.43
Heart and Vascular Diseases	Cardiomegaly	13	negative	81.09
Heart and Vascular Diseases	Cardiomyopathy	24	negative	78.89
Heart and Vascular Diseases	Dilated cardiomyopathy	7	negative	75.28
Heart and Vascular Diseases	Disorder of cardiac function	15	negative	74.89
Heart and Vascular Diseases	Shock	7	negative	74.02
Heart and Vascular Diseases	Endocarditis	2	negative	73.05
Heart and Vascular Diseases	Hypertrophic cardiomyopathy	2	negative	72.66
Heart and Vascular Diseases	Heart disease	12	negative	72.13
Heart and Vascular Diseases	Heart failure	7	positive	70.76
Heart and Vascular Diseases	Cardiovascular disease	19	negative	58.75

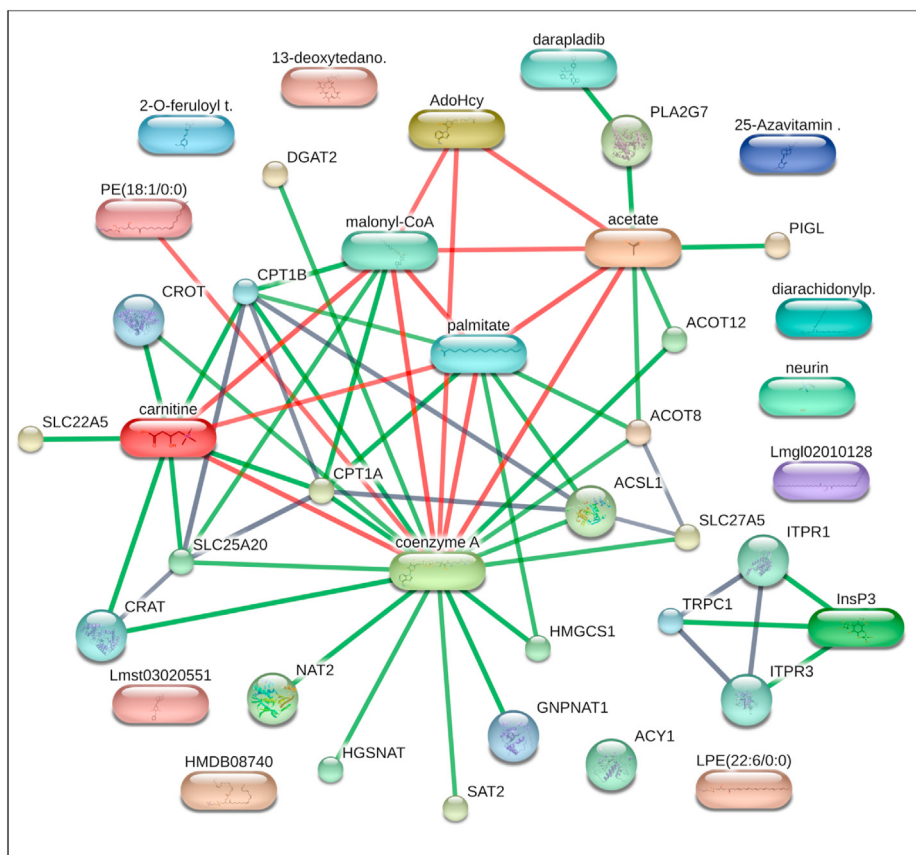


Fig. 4. Network map of predicted metabolite and associated protein of differentially expressed hepatic genes in Bitter Melon Juice (BMJ)-treated high fat diet-induced obese (DIO) C57BL/6J mice. Network mapping of significant lipid phase metabolites [PC(20:4_20:4), PC(22:6_20:4), PE(18:1), PE (22:6), 25-azavitamin D₃, 2alpha-(benzyloxy)-1alpha,25-dihydroxy-19-norvitamin D₃, 13-Deoxytedanolide, Fertaric acid, Diacylglycerol, and Neurine] detected in the plasma of BMJ + DIO mice, and metabolites (Coenzyme A, L-Carnitine, Inositol 1,4,5-trisphosphate/I3P) associated with human genes (*ACOT8*, *ACOT12*, *ACSL1*, *ACY1*, *CPT1A*, *DGAT2*, *HGSNAT*, *HMGCS1*, *NAT2*, *PIGL*, *PLA2G7*, *SAT2*, *SLC22A5*, *SLC25A20*, *SLC27A5*) were predicted to have associations based on experimental or *in silico* data using the STITCH database (<http://stitch.embl.de>). Nodes (sphere) represent a protein and splice isoform or post-translational modification. Experimental and/or predicted interactions between proteins (sphere) and chemical (cuboid) are collapsed in the map. Each node represents all the proteins produced by a single, and protein-coding gene locus. Network edges represent specific protein-protein associations jointly contribute to a shared function-but does not mean proteins physically binding each other. A small node represents that the protein 3D structure is unknown, and a large node represents a partial or full 3D structure is known or predicted. A colored node is the first shell interactor, and a white node is the second shell interactor. Connectors represent predicted associations between proteins and chemicals at high confidence (0.700). A red colored connector indicates the presence of fusion evidence. A green connector indicates neighborhood evidence. A black connector indicates co-expression evidence.

Table 5

Liquid chromatography-mass spectrometry (LC-MS) identified plasma lipid phase metabolites in Bitter Melon Juice (BMJ) treated high fat diet (HFD)- induced obese (DIO) C57BL/6J mice and key parameters. Metabolites significantly altered in the plasma of BMJ + DIO mice (FDR<0.05). n = 3 per group. Abbreviations: PC, phosphatidylcholine; PE, phosphatidylethanolamine; PS, phosphatidylserine; DG, diacylglycerol.

Metabolite	Mass (Da)	Retention time (min)	Elemental composition	Log ₂ Fold Change	FDR
PC(22:6_20:4)	853.56	5.00	C ₅₀ H ₈₀ N O ₈ P	-1.15	2.25E-02
PE(18:1)	479.31	2.16	C ₂₃ H ₄₆ N O ₇ P	-1.48	2.25E-02
Fertaric acid	308.05	0.41	C ₁₄ H ₁₄ O ₉	-2.66	2.25E-02
Neurine	85.09	0.42	C ₅ H ₁₃ N O	-1.17	2.42E-02
PE(18:1) isomer	479.31	2.16	C ₂₃ H ₄₆ N O ₇ P	-1.51	2.66E-02
25-azavitamin D ₃	384.35	4.09	C ₂₆ H ₄₃ N O	-0.73	3.33E-02
Canavalioid	545.28	1.73	C ₂₆ H ₄₂ O ₁₂	-3.13	3.33E-02
PS(17:1)	508.28	1.70	C ₂₃ H ₄₄ N O ₉ P	-1.87	3.33E-02
PC(20:4_20:4)	829.56	5.12	C ₄₈ H ₈₀ N O ₈ P	-0.82	3.81E-02
PE(22:6)	524.30	3.40	C ₂₇ H ₄₄ N O ₇ P	2.16	3.81E-02
DG(40:1)	660.61	8.08	C ₄₃ H ₈₂ O ₅	2.22	3.81E-02
13-Deoxytedanolide	593.35	2.10	C ₃₂ H ₅₀ O ₁₀	-1.00	4.20E-02
2alpha-(benzyloxy)-1alpha,25-dihydroxy-19-norvitamin D ₃	487.41	2.74	C ₃₃ H ₅₀ O ₄	-0.72	4.20E-02

Metabolite and gene interactions were also predicted between differentially expressed hepatic transcripts and plasma metabolites in BMJ-treated DIO mice *via* Enrichr (Supplemental Table 8). Metabolites (Coenzyme A, L-carnitine, Acetic acid, Inositol 1,4,5-

trisphosphate (I3P), and S-Adenosylhomocysteine) were linked to 15 human isoforms of mouse genes differentially expressed in BMJ + DIO group. Two genes, *CPT1α* and *ACOT12*, were predicted to strongly relate to coenzyme A, L-carnitine and acetic acid (Fig. 4).

Also, *Ppara*-mediated lipid metabolism (*HMGCS1*, *CPT1 α* , *SLC27A5*), peroxisome/bile acid (*ACOT8*, *ACSL1*), insulin resistance (*CPT1 α* , *SLC27A5*), DAG, triglyceride and fatty acid synthesis (*DGAT2*, *PLCG1*, *PLCB1*), β -oxidation/thermogenesis (*CPT1 α* , *ACSL1*), ER stress mediated apoptosis (*ITPR1*), and immune response, and phospholipid (*PLA2G7*) targets were predicted to interact with plasma metabolites as well; however, these interactions did not survive multiple hypothesis testing.

4. Discussion

Diet-induced obesity is a major public health concern that serves as a gateway condition to the development of undiagnosed MetS in many American adults and adolescents.^{53–55} To address this metabolic state, bitter melon-intake has been suggested as one of the alternative approaches with beneficial effects against MetS. However, studies delineating bitter melon inhibitory mechanisms against MetS analyzing both the transcriptome and metabolome under DIO state are absent; addressing this critical gap in the literature is the focus of our present study. Our findings in this pilot study show that bitter melon partially induces its metabolic effects via coordination between *Ppara* and circadian rhythm targets to modulate immune responses, and metabolic processes in glucose homeostasis, glycerophospholipid and vitamin D metabolism.

Circadian rhythmic control exists in every metabolic process and its dysregulation can disrupt the rhythmic patterns of various metabolic processes leading to the onset of MetS.^{51,56} Accumulation of abnormal metabolic signaling such as insulin insensitivity, inflammation, imbalance of adipocytokine regulation, vitamin D metabolism and glucose homeostasis contribute to MetS development.^{16,17,26,27,30,57–59} Circadian rhythm abnormalities are recognized as the overarching biological trigger for major conditions involved in MetS pathogenesis.^{51,56,60} Energy sensory proteins, PPARs^{51,61} and AMPK^{62–64} regulate circadian rhythmic signaling. PPARs heterodimerizes with retinoid X receptors (RXRs), and binds to the respective *Ppar* responsive regulatory elements (PPREs) on DNA of target genes to regulate circadian rhythm signaling.^{65,66} AMPK mediates the phosphorylation and stability of circadian-associated proteins, CRY and PER.⁶³ In circadian signaling, NAD + biosynthesis and its rate-limiting enzyme, NAMPT, are regulated by clock genes, *Clock* and *Bmal1*, by binding to the *Nampt* promoter.⁶³ Increased *Nampt* expression can activate AMPK leading to enhanced SIRT1 activity via upregulation of NAD + cellular levels.⁶³ Also, inhibition of *Clock* and *Bmal1* gene expression occurs via SIRT recruitment to the *Nampt* promoter.⁶³ Circadian dysregulation in MetS has shown a strong relationship to aberrant signaling of metabolic regulators, PPAR and AMPK, and their targets.^{63,64}

Notably, several doses of bitter melon have been shown to lower triglyceride, cholesterol and increase adiponectin plasma levels via upregulation of *Ppara*/ γ signaling and its targets *in vivo*.^{27,66,67} Bitter melon activation of AMPK has been commensurated by our lab studies^{23,24} and other reports.^{68,69} Interestingly in our study, analysis of the hepatic transcriptome after BMJ intervention in DIO mice revealed an increase in *Ppara* signaling targets, *Acs11*, *Cyp4a32*, and *Cyp7a1*, that can lead to the activation of other associated signaling such as AMPK, which is normally down-regulated in MetS-related conditions.⁷⁰ Furthermore, expression of clock machinery (*Cry1*, *Per2*), RAR-related orphan receptor gamma (*Rorc*) and NAD rate-limiting enzyme *Nampt* in circadian rhythm signaling was also enhanced in BMJ + DIO mice compared to the control DIO group in our study. Also, *Nr1d1* transcription was reduced in BMJ + DIO mice. Expression of *Cry1* and *Per2* (circadian rhythmic related genes) negatively correlates with cholesterol, waist circumference, visceral and subcutaneous adipose tissue in obese subjects⁷¹ and synchronization of serum Vitamin D levels in

diabetes.⁷² In line with these studies and this observation, circadian rhythm signaling interconnects the metabolism of lipid, Vitamin D, and cholesterol. Also, these results suggest BMJ upregulates circadian rhythm targets and its effect on these targets are inversely related to MetS-associated factors such as accumulation of cholesterol and visceral adipose tissue.

Improvement of fatty acid oxidation via inhibition of *Acc2* and enhancing *Cpt1 α* gene and protein activities has been viewed as a potential therapeutic strategy to treat MetS.^{73,74} In this study, BMJ reduced levels of obesity-associated genes (*Hmgcs1*, *Apobr*) and plasma canavalioid; whereas, it up-regulated brown-beige (*Fam195a*, *Slc25a20*), adipose tissue-associated genes (*Dgat2*, *Rorc*) and moderately increased *Cpt1 α* expression in the livers of BMJ + DIO mice. Also, the modest elevation of β -oxidation via *Cpt1 α* expression after BMJ treatment may be considered a possible anti-lipogenic effect exerted by BMJ in the liver of DIO mice compared with control DIO mice. Moreover, we observed a modest increase in diglyceride acyltransferase 2 (*Dgat2*) levels in the livers of BMJ + DIO mice. BMJ intervention resulted in an increase in the transcript levels of *Rorc*, a core clock/adipose tissue marker (by a ratio of 2.76) suggesting activation of circadian rhythmic signaling in the liver of DIO mice. *Fam195a* and *Slc25a20* were also previously identified as beige fat and brown adipocyte tissue-related markers.⁷⁵ Though, upregulation of *Dgat2* gene levels (coding for *Dgat2* protein—a critical enzymatic step in triglyceride synthesis in WAT) and other adipose tissue-related targets were observed in the current study, reduction of serum triglyceride and leptin levels as well as the stimulatory effect of BMJ on the hepatic expression of beige-brown fat, clock machinery, beta-oxidation and obesity-associated markers further supports the anti-lipogenic role of BMJ under HFD conditions. Interestingly similar to BMJ, it has been reported that 1% green tea also increases *Cpt1 α* levels in HFD-fed mice.⁷⁶ Though canavalioid has been implicated in adipose tissue function, its role in MetS has not been well studied.⁷⁷ Considering that hyperinsulinemia, hyperglycemia and hyperlipidemia contribute to MetS pathogenesis and can develop as a result of dysregulation of fatty acid oxidation mechanisms, it is plausible that natural products similar to BMJ exert their anti-MetS effects largely through the modulation of lipid metabolism. BMJ activation of AMPK in our previously published studies^{23,24} and stimulation of PPAR and circadian rhythm signaling-targets in the present study provide more insight that BMJ may serve as a therapeutic agent against metabolic abnormalities diagnosed in MetS patients.

Plasma levels of certain species of phospholipids are also significantly modulated in metabolic conditions such as obesity, cardiovascular disease and diabetes.^{78–83} BMJ showed its potential to target glycerophospholipid metabolism as evidenced by the suppression of serum PC, PE, and PS levels with the exception of PE(22:6). Previous reports have also shown that levels of lysoPC, lysoPE and lysoPC were restored following intervention treatments in HFD mice.^{84,85} This finding in BMJ + DIO mice may be as a result of PC and PE synthesis associated enzyme deficiencies as observed in other reports on phospholipid metabolism impairment,^{78,86,87} decreased cholesterol storage in CTP:phosphocholine cytidylyltransferase deficient macrophages,⁸⁸ increased insulin sensitivity in skeletal muscle cells of C57BL/6 mice⁸¹ and observed weight loss in HFD-induced obesity in phosphatidylethanolamine N-methyltransferase-deficient mice.⁸⁹ Plasma levels of diacylglycerol (DAG) were increased in BMJ + DIO mice, whereas triglyceride levels were decreased (normally, triglycerides can be produced from DAG by enzyme DGAT or via PC by phospholipase C⁹⁰). BMJ-associated high DAG levels may disrupt triglyceride biosynthesis leading to low levels in DIO mice. This is supported by another study wherein a high DAG diet reduced visceral fat, body weight, insulin and leptin circulating plasma levels in C57BL/6j mice.⁹¹

In this regard, previous studies have also reported that certain dietary constituents can interfere in the lipid synthesis/storage processes in hepatic tissues under DIO conditions.⁹² One such notable study has demonstrated that polyphenolic fraction of Citrus fruit 'Bergamot' (*Citrus bergamia* Risso et Poiteau) has the potential to target the abnormal accumulation of lipid droplets in hepatic tissues of cafeteria diet-induced rat model of MetS *via* induction of lipophagy (autophagy of lipid droplets).⁹² Bergamot-intake induced lipophagy resulted in dispersion/fragmentation of cellular lipid droplets in the hepatocytes, and the stored triglycerides/cholesterol in the smaller lipid droplets become more accessible to autophagosomes which resulted in hepatoprotective effects against cafeteria diet-induced fatty liver state.⁹² AMPK was identified as the possible key-player in Bergamot-induced lipophagy.⁹² Given that in our study we also observed smaller lipid droplets in the hepatic tissues after BMJ-intake and that AMPK upregulation and apoptosis/autophagy induction *via* bitter melon-intake has also been previously reported by us and others in certain cancers,^{23,93} there is a possibility that the hepatoprotective effects of BMJ are also partly associated with induction of lipophagy. Interestingly, autophagy induction by bitter-melon constituents has also been associated with PPAR γ activation⁹³ (as observed in the present study) which further indicates towards the link between Ppar modulation and possible induction of lipophagy by BMJ.

For glucose homeostasis, BMJ stimulated glycogen metabolism and insulin sensitivity (this effect was in line with previously reported studies).^{18,19,26,30,94,95} Also, BMJ improved insulin sensitivity *via* increasing levels of *Insr* and *Pik3r1* (glucose uptake) and *Ppp1r3b*, *Ppp1r3e* and *Gys2* (in glycogen synthesis). Acute inflammation marker, *IL6st*-which enhances pleiotropic IL6 signaling that has been implicated in glucose metabolism *via* glucose transport, was increased by BMJ. IL6 modulates insulin sensitivity *via* increase in glucose levels *via* modulation of AMPK and STAT3/MAPK signaling in skeletal muscle.⁹⁶ Interestingly, two *IL6st*-associated polymorphisms (rs715180, rs3729960) have been linked to elevated MetS-associated markers (waist circumference, triglyceride and fasting blood glucose levels) in non-diabetic subjects.⁹⁷ In this regard, bitter melon has been previously shown to modulate cell cycle and apoptotic protein levels in pancreatic cancer *via* PI3K/AKT, MAPK and AMPK signaling pathways that are critical to glucose metabolism.^{23,24}

In the context of MetS, Vitamin D deficiency *via* metabolism impairment has been shown to play a pertinent role in the regulation of several MetS risk factors.^{57,59,98–104} Both Vitamin D receptor (VDR) and PPARs can heterodimerize with RXR and in this process compete for binding to RXR-their predominant heterodimerization partner. After respective ligand binding to either VDR or PPAR and subsequent heterodimerization with RXR, the VDR and PPARs bind to their response elements (VDREs and PPREs) on target genes to influence transcription.¹⁰⁵ Interestingly, there is a VDRE in the PPAR promoter site, thus PPAR could act as a Vitamin D responding gene; this cross regulation of the VDR and PPAR signaling pathways can in turn influence their respective transcription factor/gene targets mRNA levels.¹⁰⁵ Different studies have shown that Vitamin D treatment with 1,25(OH)₂D₃ increased *Ppar γ* expression in 3T3-L1 preadipocytes,¹⁰⁴ and mice liver,⁵² and also increased insulin sensitivity under obese state^{99,106}; but its insufficiency impaired *Cpt1 α* , AMPK and circadian-related SIRT protein activities.⁵⁷ Serum levels of Vitamin D are inversely related with susceptibility to abdominal obesity¹⁰² and A1C levels¹⁰⁰; the circadian pattern of the serum levels have been also shown to influence type II diabetes in patients.⁷² In our present study, BMJ-intervention group exhibited up-regulated *Cyp7a1* in cholesterol metabolism and reduced 25-azavitamin D₃ and 2- α -

(benzyloxy)-1- α ,25-dihydroxy-19-norvitamin D₃. 25-azavitamin D₃ is a potent inhibitor of Vitamin D₃ conversion to 25(OH) D₃ in vitamin D metabolism.¹⁰⁷ Therefore, there is a possibility that BMJ enhances Vitamin D metabolism to prevent deficient vitamin D serum levels (evident by its reduction of 25-azavitamin D₃ plasma levels). Additional studies are needed to further validate this effect of BMJ on Vitamin D metabolism in MetS-associated diseases in the DIO model.

Interestingly in the current study, BMJ lowered plasma levels of anti-tumor macrolide/antibiotic, 13-Deoxytedanolide, and antioxidant feraric acid in DIO mice. It has been reported in previous studies that at low nanomolar concentrations, 13-Deoxytedanolide, a potent plasminogen activator inhibitor (PAI) inducer, exerted ribotoxic stress and cytotoxic responses in lung epithelial cells and promoted apoptosis *via* MAPK and JNK signaling in HeLa cells.^{108,109} Also, feraric acid has been shown to improve antioxidant activity, and inhibit the binding of human LDL to apolipoprotein B, a main constituent of LDL, *via* its oxidation *in vitro*.¹¹⁰ Thus, it is quite possible that the decreased levels of feraric acid as a result of BMJ feeding may still be sufficient to inhibit lipoprotein oxidation in DIO mice (considering at micromolar concentrations it inhibits more than 60% of human LDL oxidation). However, to date, the biological role of feraric acid has not been well studied in MetS. Additional studies to elucidate the mechanistic role of the plasma metabolites shown in the present study will be required to understand how the individual and combined effects of these metabolites impact MetS development.

Furthermore, studies show that metabolic dysregulation trigger immune response defense mechanisms such as pro-inflammatory, adipocytokine signaling and immune cell recruitment in MetS development.^{111–113} Reports have shown bitter melon increased superoxide dismutase activity¹¹⁴ and attenuated pro-inflammatory signaling in myocardial infarction, mitochondrial oxidation and HFD or other biological agents (ethanol, lipopolysaccharide, bacterial) induced neuroinflammation, and macrophage/mast cell infiltration in mice.^{17,26,115–118} Briefly, our results show BMJ intervention has an expansive influence on immunity signaling as indicated by its targeting of innate/adaptive (GO 0045087, GO 0002460), humoral immune (GO 0006959) and general immune activation (GO 0002253) responses to combat pro-inflammatory mediators involved in adipocytokine signaling. Specifically, our study results showed that BMJ leads to inhibition of pro-inflammatory cytokine (*Ccl2*), and higher levels of DG(40:1) (adipocytokine-associated metabolite). Serum analysis corroborated this observation as BMJ intervention was found to modulate adipocytokine signaling as indicated by reduction in leptin and concurrent up-regulation of adiponectin levels.

5. Conclusion

In conclusion, our in-depth transcriptomics and metabolomics analysis suggests that BMJ mediates its metabolic effects partly through modulation of *Ppara γ* signaling and its downstream targets in circadian rhythm processes to prevent excessive lipogenesis, maintain glucose homeostasis, modify immune responses signaling in diet induced MetS (Fig. 5). Furthermore, BMJ stimulation of steroid metabolic targets and suppression of inhibitor, 25-azavitamin D₃, may lead to enhanced Vitamin D metabolism in the DIO murine model. Since BMJ remains a widely consumed nutraceutical worldwide due to its effects that counteract various metabolic-associated disorders, additional mechanistic studies focused on these identified pathways are required to further establish their integrated correlations with BMJ protective benefits against MetS.

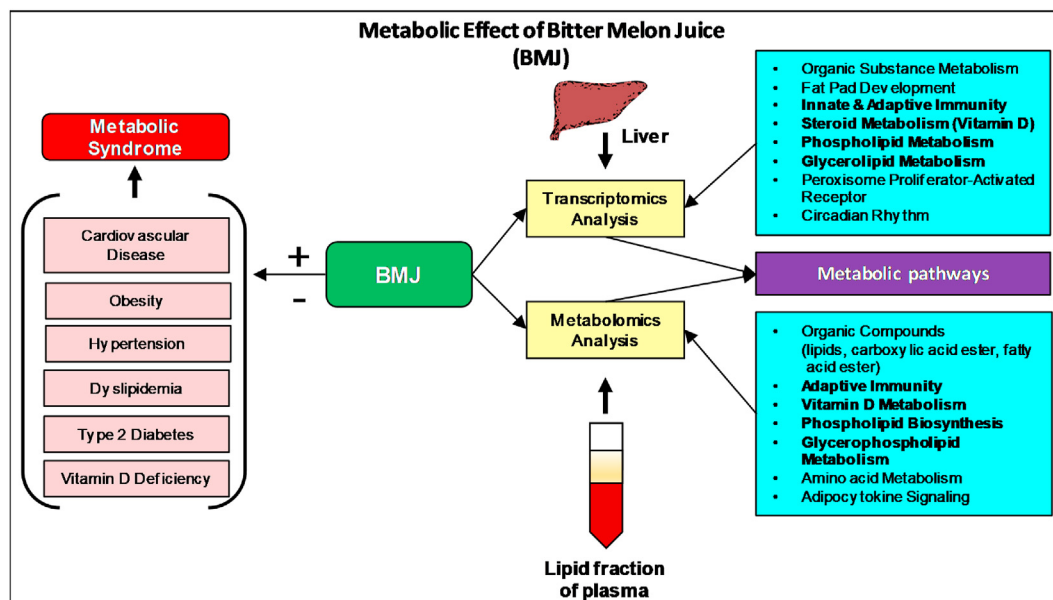


Fig. 5. Scheme depicting Bitter Melon Juice (BMJ) targeted pathways and their implications in Metabolic Syndrome (MetS). The metabolic effect of BMJ in diet-induced obese (DIO) C57BL/6J mice were determined by transcriptomics ($n = 4$ per group) and metabolomics analyses ($n = 3$ per group). Transcripts and metabolites differentially expressed in the liver and plasma lipid-phase of BMJ + DIO mice identified several common metabolic mechanisms. In the liver transcriptome and plasma metabolites, BMJ induced expression of genes and modulated levels of metabolites involved in adaptive immunity, steroid (Vitamin D), and glycerophospholipid metabolism. In addition to these pathways, peroxisome proliferator-activated receptor (PPAR), circadian rhythmic, and adipocytokine signaling which are associated with metabolic syndrome (MetS) and associated conditions (shown on the right above) are also modulated by bitter melon. Based on *in vitro* and *in vivo* models in the literature, it could be inferred that BMJ may exerts its anti-diabetic, anti-MetS and anti-inflammatory activity and other beneficial health effects via the activation of PPAR γ and AMPK signaling.

Data availability statement

Array data is available from the GEO repository (<http://www.ncbi.nlm.nih.gov/geo>) under the accession number GSE175966. The raw metabolomics data is publicly available through Metabolomics Workbench at <https://www.metabolomicsworkbench.org> with study ID ST001911, project ID PR001205 and associated doi 10.21228/M8Z700.

Declaration of competing interest

None.

Acknowledgement

The authors acknowledge the assistance of Jenny Yu (laboratory Manager-Tabakoff Lab) in RNA/array associated wet-lab techniques.

Appendix A. Supplementary data

Supplementary data to this article can be found online at <https://doi.org/10.1016/j.jtcme.2021.08.011>

Financial Support

This work was supported by the National Institutes of Health/ National Cancer Institute grant R01CA195708, the National Institutes of Health Office of Dietary Supplements supplemental funds R01CA195708-02S1, and the pilot funding from the office of the Associate Dean for Research and Graduate Education (ADR), School of Pharmacy, UC-AMC (to RA), and the National Cancer Institute diversity supplement grant R01CA195708-04S1 (to DR and RA).

References

- Mendrick DL, Diehl AM, Topor LS, et al. Metabolic syndrome and associated diseases: from the bench to the clinic. *Toxicol Sci.* 2018;162(1):36–42.
- Taylor JY, Kraja AT, de Las Fuentes L, Stanfill AG, Clark A, Cashion A. An overview of the genomics of metabolic syndrome. *J Nurs Scholarsh : an official publication of Sigma Theta Tau International Honor Society of Nursing.* 2013;45(1):52–59.
- Ford ES, Li C, Zhao G. Prevalence and correlates of metabolic syndrome based on a harmonious definition among adults in the US. *J Diabetes.* 2010;2(3):180–193.
- National Center for Health Statistics (U.S.). NCHS Data Brief. Hyattsville, MD: National Center for Health Statistics:volumes.
- Third report of the national cholesterol education Program (NCEP) expert panel on detection, evaluation, and treatment of high blood cholesterol in adults (adult treatment panel III) final report. *Circulation.* 2002;106(25):3143–3421.
- Grundy SM, Cleeman JJ, Daniels SR, et al. Diagnosis and management of the metabolic syndrome: an American heart association/national heart, lung, and blood Institute scientific statement. *Circulation.* 2005;112(17):2735–2752.
- Sperling LS, Mechanick JJ, Neeland JJ, et al. The CardioMetabolic health alliance: working toward a new Care model for the metabolic syndrome. *J Am Coll Cardiol.* 2015;66(9):1050–1067.
- Zimmet P, Magliano D, Matsuzawa Y, Alberti G, Shaw J. The metabolic syndrome: a global public health problem and a new definition. *J Atherosclerosis Thromb.* 2005;12(6):295–300.
- Huang PL. A comprehensive definition for metabolic syndrome. *Disease models & mechanisms.* 2009;2(5-6):231–237.
- de Toro-Martín J, Arsenault BJ, Despres JP, Vohl MC. Precision nutrition: a review of personalized nutritional approaches for the prevention and management of metabolic syndrome. *Nutrients.* 2017;9(8).
- Patti AM, Al-Rasadi K, Giglio RV, et al. Natural approaches in metabolic syndrome management. *Arch Med Sci.* 2018;14(2):422–441.
- Chaiwong S, Chatturong U, Chanasong R, et al. Dried mulberry fruit ameliorates cardiovascular and liver histopathological changes in high-fat diet-induced hyperlipidemic mice. *Journal of traditional and complementary medicine.* 2021;11(4):356–368.
- Khatun MA, Sato S, Konishi T. Obesity preventive function of novel edible mushroom, Basidiomycetes-X (Echigoshirayukidake): manipulations of insulin resistance and lipid metabolism. *Journal of traditional and complementary medicine.* 2020;10(3):245–251.
- Waltenberger B, Mocan A, Smejkal K, Heiss EH, Atanasov AG. Natural products to counteract the epidemic of cardiovascular and metabolic disorders. *Molecules.* 2016;21(6).
- Raina K, Kumar D, Agarwal R. Promise of bitter melon (*Momordica charantia*)

- bioactives in cancer prevention and therapy. *Semin Canc Biol.* 2016;40–41:116–129.
16. Mahwish Saeed F, Arshad MS, Nisa MU, Nadeem MT, Arshad MU. Hypoglycemic and hypolipidemic effects of different parts and formulations of bitter melon (*Momordica Charantia*). *Lipids Health Dis.* 2017;16(1):211.
 17. Bao B, Chen YG, Zhang L, et al. *Momordica charantia* (Bitter Melon) reduces obesity-associated macrophage and mast cell infiltration as well as inflammatory cytokine expression in adipose tissues. *PLoS One.* 2013;8(12):e84075.
 18. Selvakumar G, Shathirapathy G, Jainraj R, Yuvaraj Paul P. Immediate effect of bitter melon seed, ash gourd, Knol-khol juices on blood sugar levels of patients with type 2 diabetes mellitus: a pilot study. *Journal of traditional and complementary medicine.* 2017;7(4):526–531.
 19. Krawinkel MB, Ludwig C, Swai ME, Yang RY, Chun KP, Habicht SD. Bitter melon reduces elevated fasting plasma glucose levels in an intervention study among prediabetics in Tanzania. *J Ethnopharmacol.* 2018;216:1–7.
 20. Tsai CH, Chen EC, Tsay HS, Huang CJ. Wild bitter melon improves metabolic syndrome: a preliminary dietary supplementation trial. *Nutr J.* 2012;11:4.
 21. Chen GC, Su HM, Lin YS, Tsou PY, Chyuan JH, Chao PM. A conjugated fatty acid present at high levels in bitter melon seed favorably affects lipid metabolism in hepatocytes by increasing NAD(+)/NADH ratio and activating PPARalpha, AMPK and SIRT1 signaling pathway. *J Nutr Biochem.* 2016;33:28–35.
 22. Gadang V, Gilbert W, Hettiarachchi N, Horax R, Katwa L, Devareddy L. Dietary bitter melon seed increases peroxisome proliferator-activated receptor-gamma gene expression in adipose tissue, down-regulates the nuclear factor-kappaB expression, and alleviates the symptoms associated with metabolic syndrome. *J Med Food.* 2011;14(1-2):86–93.
 23. Kaur M, Deep G, Jain AK, et al. Bitter melon juice activates cellular energy sensor AMP-activated protein kinase causing apoptotic death of human pancreatic carcinoma cells. *Carcinogenesis.* 2013;34(7):1585–1592.
 24. Somasagara RR, Deep G, Shrotriya S, Patel M, Agarwal C, Agarwal R. Bitter melon juice targets molecular mechanisms underlying gemcitabine resistance in pancreatic cancer cells. *Int J Oncol.* 2015;46(4):1849–1857.
 25. Bakare RI, Magbagbeola OA, Akinwande AI, Okunowo OW. Nutritional and chemical evaluation of *Momordica charantia*. *J Med Plants Res.* 2010;4(21):2189–2193.
 26. Yang SJ, Choi JM, Park SE, et al. Preventive effects of bitter melon (*Momordica charantia*) against insulin resistance and diabetes are associated with the inhibition of NF-kappaB and JNK pathways in high-fat-fed OLETF rats. *J Nutr Biochem.* 2015;26(3):234–240.
 27. Chao CY, Yin MC, Huang CJ. Wild bitter melon extract up-regulates mRNA expression of PPARalpha, PPARgamma and their target genes in C57BL/6J mice. *J Ethnopharmacol.* 2011;135(1):156–161.
 28. Chen Q, Li ET. Reduced adiposity in bitter melon (*Momordica charantia*) fed rats is associated with lower tissue triglyceride and higher plasma catecholamines. *Br J Nutr.* 2005;93(5):747–754.
 29. Chen GC, Chen WH, Tseng KT, Chao PM. The anti-adiposity effect of bitter melon seed oil is solely attributed to its fatty acid components. *Lipids Health Dis.* 2017;16(1):186.
 30. Ooi CP, Yassin Z, Hamid TA. *Momordica charantia* for type 2 diabetes mellitus. *Cochrane Database Syst Rev.* 2010;(2):CD007845.
 31. Dhar D, Raina K, Agarwal R. Mechanisms and drug targets for pancreatic cancer chemoprevention. *Curr Med Chem.* 2018;25(22):2545–2565.
 32. Dhar D, Raina K, Kant R, et al. Bitter melon juice-intake modulates glucose metabolism and lactate efflux in tumors in its efficacy against pancreatic cancer. *Carcinogenesis.* 2019;40(9):1164–1176. <https://doi.org/10.1093/carcin/bgz114>. pii: bgz114.
 33. Dhar D, Raina K, Kumar D, et al. Bitter melon juice intake with gemcitabine intervention circumvents resistance to gemcitabine in pancreatic patient-derived xenograft tumors. *Mol Carcinog.* 2020;59(10):1227–1240.
 34. Vanderlinden LA, Saba LM, Bennett B, Hoffman PL, Tabakoff B. Influence of sex on genetic regulation of "drinking in the dark" alcohol consumption. *Mamm Genome : official journal of the International Mammalian Genome Society.* 2015;26(1-2):43–56.
 35. Shakya K, Ruskin HJ, Kerr G, Crane M, Becker J. Comparison of microarray preprocessing methods. *Adv Exp Med Biol.* 2010;680:139–147.
 36. Yang Y, Cruickshank C, Armstrong M, Mahaffey S, Reisdorph N. New sample preparation approach for mass spectrometry-based profiling of plasma results in improved coverage of metabolome. *J Chromatogr A.* 2013;1300:217–226.
 37. Cruickshank-Quinn C, Quinn KD, Powell R, et al. Multi-step preparation technique to recover multiple metabolite compound classes for in-depth and informative metabolomic analysis. *JoVE : JoVE.* 2014;89.
 38. Bahr TM, Hughes GJ, Armstrong M, et al. Peripheral blood mononuclear cell gene expression in chronic obstructive pulmonary disease. *Am J Respir Cell Mol Biol.* 2013;49(2):316–323.
 39. Sun W, Kechris K, Jacobson S, et al. Common genetic polymorphisms influence blood biomarker measurements in COPD. *PLoS Genet.* 2016;12(8):e1006011.
 40. Redestig H, Fukushima A, Stenlund H, et al. Compensation for systematic cross-contribution improves normalization of mass spectrometry based metabolomics data. *Anal Chem.* 2009;81(19):7974–7980.
 41. Hughes G, Cruickshank-Quinn C, Reisdorph R, et al. MSprep—summarization, normalization and diagnostics for processing of mass spectrometry-based metabolomic data. *Bioinformatics.* 2014;30(1):133–134.
 42. NIST. NIST/EPA/NIH mass spectral library with search Program (data version: NIST 14, software version 2.2g). <http://www.nist.gov/srd/nist1a.cfm>; 2014.
 43. Oba S, Sato MA, Takemasa I, Monden M, Matsubara K, Ishii S. A Bayesian missing value estimation method for gene expression profile data. *Bioinformatics.* 2003;19(16):2088–2096.
 44. Chen EY, Tan CM, Kou Y, et al. Enrichr: interactive and collaborative HTML5 gene list enrichment analysis tool. *BMC Bioinf.* 2013;14:128.
 45. Kuleshov MV, Jones MR, Rouillard AD, et al. Enrichr: a comprehensive gene set enrichment analysis web server 2016 update. *Nucleic Acids Res.* 2016;44(W1):W90–W97.
 46. Szklarczyk D, Santos A, von Mering C, Jensen LJ, Bork P, Kuhn M. STITCH 5: augmenting protein-chemical interaction networks with tissue and affinity data. *Nucleic Acids Res.* 2016;44(D1):D380–D384.
 47. Kupersmidt I, Su QJ, Grewal A, et al. Ontology-based meta-analysis of global collections of high-throughput public data. *PLoS One.* 2010;5(9).
 48. Lopez-Ibanez J, Pazos F, Chagoyen M. MBOLE 2.0-functional enrichment of chemical compounds. *Nucleic Acids Res.* 2016;44(W1):W201–W204.
 49. Smyth GK. *Linear Models and Empirical Bayes Methods for Assessing Differential Expression in Microarray Experiments. Statistical Applications in Genetics and Molecular Biology.* vol. 3. Article3; 2004.
 50. Verreth W, De Keyser D, Pelat M, et al. Weight-loss-associated induction of peroxisome proliferator-activated receptor-alpha and peroxisome proliferator-activated receptor-gamma correlate with reduced atherosclerosis and improved cardiovascular function in obese insulin-resistant mice. *Circulation.* 2004;110(20):3259–3269.
 51. Charoensuksai P, Xu W. PPARs in rhythmic metabolic regulation and implications in health and disease. *PPAR Res.* 2010;2010.
 52. Hoseini R, Damirchi A, Babaei P. Vitamin D increases PPARgamma expression and promotes beneficial effects of physical activity in metabolic syndrome. *Nutrition.* 2017;36:54–59.
 53. Hales CM, Carroll MD, Fryar CD, Ogden CL. *Prevalence of Obesity Among Adults and Youth: United States, 2015–2016.* Hyattsville, MD: National Center for Health Statistics; 2017.
 54. Hales CM, Carroll MD, Fryar CD, Ogden CL. *Prevalence of Obesity and Severe Obesity Among Adults: United States, 2017–2018.* Hyattsville, MD: National Center for Health Statistics; 2020.
 55. Moore JX, Chaudhary N, Akinemiju T. Metabolic syndrome prevalence by race/ethnicity and sex in the United States, national health and nutrition examination survey, 1988–2012. *Prev Chronic Dis.* 2017;14:E24.
 56. Maury E, Ramsey KM, Bass J. Circadian rhythms and metabolic syndrome: from experimental genetics to human disease. *Circ Res.* 2010;106(3):447–462.
 57. Chang E, Kim Y. Vitamin D insufficiency exacerbates adipose tissue macrophage infiltration and decreases AMPK/SIRT1 activity in obese rats. *Nutrients.* 2017;9(4).
 58. Anderson JL, May HT, Horne BD, et al. Relation of vitamin D deficiency to cardiovascular risk factors, disease status, and incident events in a general healthcare population. *Am J Cardiol.* 2010;106(7):963–968.
 59. Awad AB, Alappat L, Valerio M. Vitamin D and metabolic syndrome risk factors: evidence and mechanisms. *Crit Rev Food Sci Nutr.* 2012;52(2):103–112.
 60. Zimmet P, Alberti K, Stern N, et al. The circadian syndrome: is the metabolic syndrome and much more!. *J Intern Med.* 2019;286(2):181–191.
 61. Marciano DP, Chang MR, Corzo CA, et al. The therapeutic potential of nuclear receptor modulators for treatment of metabolic disorders: PPARgamma, RORs, and Rev-erbs. *Cell Metabol.* 2014;19(2):193–208.
 62. Kahn BB, Alquier T, Carling D, Hardie DG. AMP-activated protein kinase: ancient energy gauge provides clues to modern understanding of metabolism. *Cell Metabol.* 2005;1(1):15–25.
 63. Jordan SD, Lamia KA, AMPK at the crossroads of circadian clocks and metabolism. *Mol Cell Endocrinol.* 2013;366(2):163–169.
 64. Lamia KA, Sachdeva UM, DiTacchio L, et al. AMPK regulates the circadian clock by cryptochrome phosphorylation and degradation. *Science.* 2009;326(5951):437–440.
 65. Corrales P, Vidal-Puig A, Medina-Gomez G. PPARs and metabolic disorders associated with challenged adipose tissue plasticity. *Int J Mol Sci.* 2018;19(7).
 66. Ahmadian M, Suh JM, Hah N, et al. PPARgamma signaling and metabolism: the good, the bad and the future. *Nat Med.* 2013;19(5):557–566.
 67. Wang J, Ryu HK. The effects of *Momordica charantia* on obesity and lipid profiles of mice fed a high-fat diet. *Nutr Res Pract.* 2015;9(5):489–495.
 68. Shih CC, Shih MT, Lin CH, Wu JB. *Momordica charantia* ameliorates insulin resistance and dyslipidemia with altered hepatic glucose production and fatty acid synthesis and AMPK phosphorylation in high-fat-fed mice. *Phytother Res.* 2014;28(3):363–371.
 69. Yung MM, Ross FA, Hardie DG, et al. Bitter melon (*Momordica charantia*) extract inhibits tumorigenicity and overcomes cisplatin-resistance in ovarian cancer cells through targeting AMPK signaling cascade. *Integr Canc Ther.* 2016;15(3):376–389.
 70. Ruderman NB, Carling D, Prentki M, Cacicedo JM. AMPK, insulin resistance, and the metabolic syndrome. *J Clin Invest.* 2013;123(7):2764–2772.
 71. Gomez-Abellan P, Hernandez-Morante JJ, Lujan JA, Madrid JA, Garaulet M. Clock genes are implicated in the human metabolic syndrome. *Int J Obes.* 2008;32(1):121–128.
 72. Masood T, Kushwaha RS, Singh R, et al. Circadian rhythm of serum 25 (OH) vitamin D, calcium and phosphorus levels in the treatment and management of type-2 diabetic patients. *Drug Discov Ther.* 2015;9(1):70–74.
 73. Schreurs M, Kuipers F, van der Leij FR. Regulatory enzymes of mitochondrial beta-oxidation as targets for treatment of the metabolic syndrome. *Obes Rev.*

- 2010;11(5):380–388.
74. Wakil SJ, Abu-Elheiga LA. Fatty acid metabolism: target for metabolic syndrome. *J Lipid Res.* 2009;50(Suppl):S138–S143.
 75. Xue H, Wang Z, Hua Y, et al. Molecular signatures and functional analysis of beige adipocytes induced from in vivo intra-abdominal adipocytes. *Sci Adv.* 2018;4(7):eaar5319.
 76. Lee LS, Choi JH, Sung MJ, et al. Green tea changes serum and liver metabolomic profiles in mice with high-fat diet-induced obesity. *Mol Nutr Food Res.* 2015;59(4):784–794.
 77. Murakami T, Kohno K, Kishi A, Matsuda H, Yoshikawa M. Medicinal foodstuffs. XIX. Absolute stereostructures of canavalioides, a new Ent-kaurane-type diterpene glycoside, and gladiatoides A1, A2, A3, B1, B2, B3, C1, and C2, new acylated flavonol glycosides, from sword bean, the seeds of *Canavalia gladiata*. *Chem Pharm Bull (Tokyo).* 2000;48(11):1673–1680.
 78. Del Bas JM, Caimari A, Rodriguez-Naranjo MI, et al. Impairment of lysophospholipid metabolism in obesity: altered plasma profile and desensitization to the modulatory properties of n-3 polyunsaturated fatty acids in a randomized controlled trial. *Am J Clin Nutr.* 2016;104(2):266–279.
 79. Salatzki J, Foryst-Ludwig A, Bentele K, et al. Adipose tissue ATGL modifies the cardiac lipidome in pressure-overload-induced left ventricular failure. *PLoS Genet.* 2018;14(1), e1007171.
 80. Kim HJ, Kim JH, Noh S, et al. Metabolomic analysis of livers and serum from high-fat diet induced obese mice. *J Proteome Res.* 2011;10(2):722–731.
 81. Funai K, Lodhi JJ, Spears LD, et al. Skeletal muscle phospholipid metabolism regulates insulin sensitivity and contractile function. *Diabetes.* 2016;65(2):358–370.
 82. Barber MN, Risis S, Yang C, et al. Plasma lysophosphatidylcholine levels are reduced in obesity and type 2 diabetes. *PLoS One.* 2012;7(7), e41456.
 83. Lee HS, Nam Y, Chung YH, et al. Beneficial effects of phosphatidylcholine on high-fat diet-induced obesity, hyperlipidemia and fatty liver in mice. *Life Sci.* 2014;118(1):7–14.
 84. Nam M, Choi MS, Choi JY, et al. Effect of green tea on hepatic lipid metabolism in mice fed a high-fat diet. *J Nutr Biochem.* 2018;51:1–7.
 85. Vial G, Chauvin MA, Bendridi N, et al. Imeglimin normalizes glucose tolerance and insulin sensitivity and improves mitochondrial function in liver of a high-fat, high-sucrose diet mice model. *Diabetes.* 2015;64(6):2254–2264.
 86. Walkey CJ, Yu L, Agellon LB, Vance DE. Biochemical and evolutionary significance of phospholipid methylation. *J Biol Chem.* 1998;273(42):27043–27046.
 87. van der Veen JN, Lingrell S, McCloskey N, et al. A role for phosphatidylcholine and phosphatidylethanolamine in hepatic insulin signaling. *Faseb J.* 2019;33(4):5045–5057.
 88. Zhang D, Tang W, Yao PM, et al. Macrophages deficient in CTP:Phosphocholine cytidyltransferase- α are viable under normal culture conditions but are highly susceptible to free cholesterol-induced death. Molecular genetic evidence that the induction of phosphatidylcholine biosynthesis in free cholesterol-loaded macrophages is an adaptive response. *J Biol Chem.* 2000;275(45):35368–35376.
 89. Jacobs RL, Zhao Y, Koonen DP, et al. Impaired de novo choline synthesis explains why phosphatidylethanolamine N-methyltransferase-deficient mice are protected from diet-induced obesity. *J Biol Chem.* 2010;285(29):22403–22413.
 90. van der Veen JN, Kennelly JP, Wan S, Vance JE, Vance DE, Jacobs RL. The critical role of phosphatidylcholine and phosphatidylethanolamine metabolism in health and disease. *Biochim Biophys Acta Biomembr.* 2017;1859(9 Pt B):1558–1572.
 91. Murase T, Mizuno T, Omachi T, et al. Dietary diacylglycerol suppresses high fat and high sucrose diet-induced body fat accumulation in C57BL/6j mice. *J Lipid Res.* 2001;42(3):372–378.
 92. Parafati M, Lascala A, Morittu VM, et al. Bergamot polyphenol fraction prevents nonalcoholic fatty liver disease via stimulation of lipophagy in cafeteria diet-induced rat model of metabolic syndrome. *J Nutr Biochem.* 2015;26(9):938–948.
 93. Weng JR, Bai LY, Chiu CF, Hu JL, Chiu SJ, Wu CY. Cucurbitane triterpenoid from *Momordica charantia* induces apoptosis and autophagy in breast cancer cells, in part, through peroxisome proliferator-activated receptor gamma activation. *Evid Based Complement Alternat Med.* 2013;2013:935675.
 94. Cortez-Navarrete M, Martinez-Abundis E, Perez-Rubio KG, Gonzalez-Ortiz M, Mendez-Del Villar M. *Momordica charantia* administration improves insulin secretion in type 2 diabetes mellitus. *J Med Food.* 2018;21(7):672–677.
 95. Singh J, Cumming E, Manoharan G, Kalasz H, Adeghate E. Medicinal chemistry of the anti-diabetic effects of *Momordica charantia*: active constituents and modes of actions. *Open Med Chem J.* 2011;5(Suppl 2):70–77.
 96. Glund S, Deshmukh A, Long YC, et al. Interleukin-6 directly increases glucose metabolism in resting human skeletal muscle. *Diabetes.* 2007;56(6):1630–1637.
 97. Gottardo L, De Cosmo S, Zhang YY, et al. A polymorphism at the IL6ST (gp130) locus is associated with traits of the metabolic syndrome. *Obesity.* 2008;16(1):205–210.
 98. Prasad P, Kochhar A. Interplay of vitamin D and metabolic syndrome: a review. *Diabetes Metab Syndr.* 2016;10(2):105–112.
 99. Pramono A, Jocken JWE, Essers YPG, Goossens GH, Blaak EE. Vitamin D and tissue-specific insulin sensitivity in humans with overweight/obesity. *J Clin Endocrinol Metab.* 2019;104(1):49–56.
 100. Dalgard C, Petersen MS, Weihe P, Grandjean P. Vitamin D status in relation to glucose metabolism and type 2 diabetes in septuagenarians. *Diabetes Care.* 2011;34(6):1284–1288.
 101. Mozos I, Marginean O. Links between vitamin D deficiency and cardiovascular diseases. *BioMed Res Int.* 2015;2015:109275.
 102. Mansouri M, Abasi R, Nasiri M, et al. Association of vitamin D status with metabolic syndrome and its components: a cross-sectional study in a population of high educated Iranian adults. *Diabetes Metab Syndr.* 2018;12(3):393–398.
 103. Zhuang H, Lin Y, Yang G. Effects of 1,25-dihydroxyvitamin D3 on proliferation and differentiation of porcine preadipocyte in vitro. *Chem Biol Interact.* 2007;170(2):114–123.
 104. Kong J, Li YC. Molecular mechanism of 1,25-dihydroxyvitamin D3 inhibition of adipogenesis in 3T3-L1 cells. *Am J Physiol Endocrinol Metab.* 2006;290(5):E916–E924.
 105. Matsuda S, Kitagishi Y. Peroxisome proliferator-activated receptor and vitamin d receptor signaling pathways in cancer cells. *Cancers.* 2013;5(4):1261–1270.
 106. Hanafy AS, Elkatawy HA. Beneficial effects of vitamin D on insulin sensitivity, blood pressure, abdominal subcutaneous fat thickness, and weight loss in refractory obesity. *Clin Diabetes.* 2018;36(3):217–225.
 107. Onisko BL, Schnoes HK, DeLuca HF. 25-Azavitamin D3, an inhibitor of vitamin D metabolism and action. *J Biol Chem.* 1979;254(9):3493–3496.
 108. Lee KH, Nishimura S, Matsunaga S, et al. Induction of a ribotoxic stress response that stimulates stress-activated protein kinases by 13-deoxytetraolide, an antitumor marine macrolide. *Biosci Biotechnol Biochem.* 2006;70(1):161–171.
 109. Schroeder SJ, Blaha G, Tirado-Rives J, Steitz TA, Moore PB. The structures of antibiotics bound to the E site region of the 50 S ribosomal subunit of *Halorubra marismortui*: 13-deoxytetraolide and girodazole. *J Mol Biol.* 2007;367(5):1471–1479.
 110. Meyer AS, Donovan JL, Pearson DA, Waterhouse AL, Frankel EN. Fruit hydroxycinnamic acids inhibit human low-density lipoprotein oxidation in vitro. *J Agric Food Chem.* 1998;46(5):1783–1787.
 111. Avtanski D, Pavlov VA, Tracey KJ, Poretsky L. Characterization of inflammation and insulin resistance in high-fat diet-induced male C57BL/6j mouse model of obesity. *Animal Model Exp Med.* 2019;2(4):252–258.
 112. van der Heijden RA, Sheedfar F, Morrison MC, et al. High-fat diet induced obesity primes inflammation in adipose tissue prior to liver in C57BL/6j mice. *Aging (N Y).* 2015;7(4):256–268.
 113. Kadowaki T, Yamauchi T, Kubota N, Hara K, Ueki K, Tobe K. Adiponectin and adiponectin receptors in insulin resistance, diabetes, and the metabolic syndrome. *J Clin Invest.* 2006;116(7):1784–1792.
 114. Xu J, Cao K, Li Y, et al. Bitter melon inhibits the development of obesity-associated fatty liver in C57BL/6 mice fed a high-fat diet. *J Nutr.* 2014;144(4):475–483.
 115. Nerurkar PV, Johns LM, Buesa LM, et al. *Momordica charantia* (bitter melon) attenuates high-fat diet-associated oxidative stress and neuroinflammation. *J Neuroinflammation.* 2011;8:64.
 116. Raish M. *Momordica charantia* polysaccharides ameliorate oxidative stress, hyperlipidemia, inflammation, and apoptosis during myocardial infarction by inhibiting the NF- κ B signaling pathway. *Int J Biol Macromol.* 2017;97:544–551.
 117. Alam MA, Uddin R, Subhan N, Rahman MM, Jain P, Reza HM. Beneficial role of bitter melon supplementation in obesity and related complications in metabolic syndrome. *Journal of lipids.* 2015;2015:496169.
 118. Jang S-W, Lim S-G, Lee D-S, Suk K, Lee W-H. Fermented bitter melon extract differentially regulates lipopolysaccharide-induced cytokine gene expression through nuclear factor- κ B and interferon regulatory factor-1. *Anim Cell Syst.* 2015;19(3):194–200.